AD-A087 289 PENNSYLVANIA UNIV PHILADELPHIA F/G 11/9
ELECTRICAL TRANSPORT IN DOPED POLYACETYLENE.(U)
JUL 80 Y - PARK, A J HEEGER, M A DRUY N00014-75-C-0962
UNCLASSIFIED TR-80-4 NL

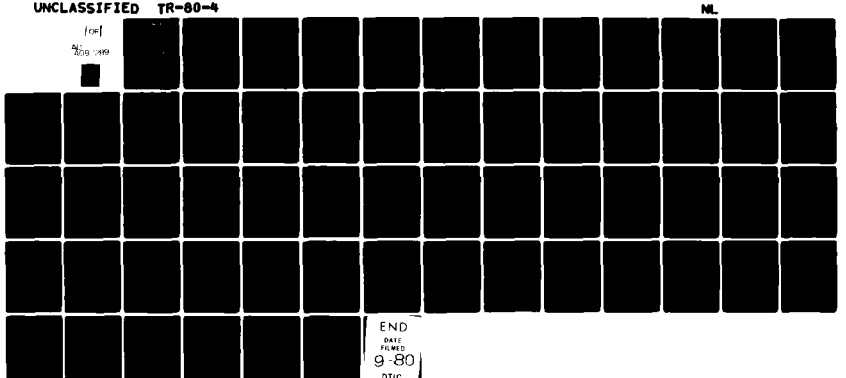

END
DATE FILMED
9-80
DTIC

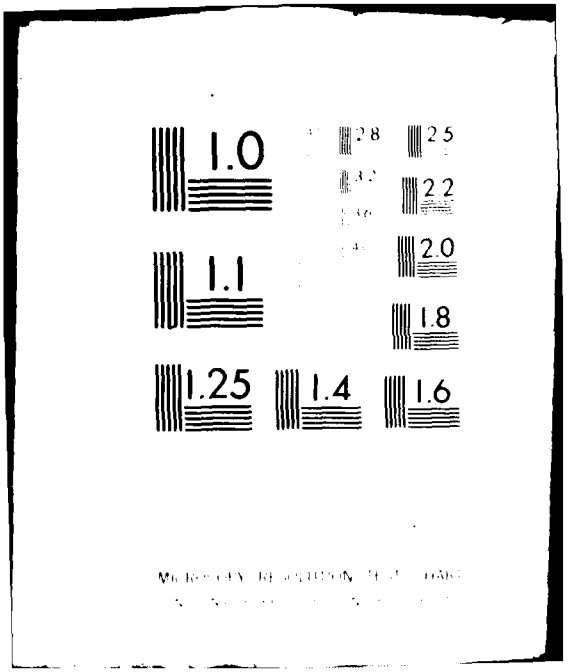
1.0
1.1
1.25
1.4
1.6
2.0
1.8
2.2
2.5

Unclassified

SECURITY CLASSIFICATION OF THIS PAGE (When Data Entered)

LEVEL II

REPORT DOCUMENTATION PAGE

READ INSTRUCTIONS BEFORE COMPLETING FORM

1. REPORT NUMBER	2. GOVT ACCESSION NO.	3. RECIPIENT'S CATALOG NUMBER
Technical Report 80-4	AD-A087289	TR-87-4

4. TITLE (and Subtitle)

Electrical Transport in Doped Polyacetylene

5. TYPE OF REPORT & PERIOD COVERED

Interim Technical Report

6. PERFORMING ORG. REPORT NUMBER

7. AUTHOR(s)

Y.-W. Park, A. J. Heeger, M. A. Druy and A. G. MacDiarmid

8. CONTRACT OR GRANT NUMBER(s)

N00014-75-C-0962, NSF-DMR76-80974

9. PERFORMING ORGANIZATION NAME AND ADDRESS

Departments of Physics and Chemistry*
University of Pennsylvania
Philadelphia, Pa. 19104

10. PROGRAM ELEMENT, PROJECT, TASK AREA & WORK UNIT NUMBERS

NR-356-602

11. CONTROLLING OFFICE NAME AND ADDRESS

Department of the Navy
Office of Naval Research
Arlington, Va. 22217

12. REPORT DATE

July 8, 1980

13. NUMBER OF PAGES

54

14. MONITORING AGENCY NAME & ADDRESS(if different from Controlling Office)

15. SECURITY CLASS. (of this report)

Unclassified

15a. DECLASSIFICATION/DOWNGRADING SCHEDULE

16. DISTRIBUTION STATEMENT (of this Report)

Distribution unlimited; approved for public release

DTIC ELECTE JUL 30 1980 S D E

17. DISTRIBUTION STATEMENT (of the abstract entered in Block 20, if different from Report)

18. SUPPLEMENTARY NOTES

Prepared for publication in J. Chem. Phys.

19. KEY WORDS (Continue on reverse side if necessary and identify by block number)

transport, polyacetylene, conductivity, thermopower, semiconductor, metal, transition, mobility, solitons, polyene, anisotropic, oriented, hopping, oriented films, dilute limit, transitional region, metallic state, carrier, charge transfer, band theory, delocalized states, disordered polymer, metallic strands, potential barriers

20. ABSTRACT (Continue on reverse side if necessary and identify by block number)

The results of an experimental study of electrical conductivity and thermopower in doped polyacetylene are reported. Included are measurements on both as-grown and partially oriented films doped with iodine and AsF_5; $[CH(AsF_5)_y]_x$ and $[CH(I_3)_y]_x$, where y covers the full doping range. The data indicate three important concentration regimes; the dilute limit ($y<0.001$), the transitional region ($0.001<y<0.01$), and the metallic state ($y>0.01$). In the dilute limit, the transport is via carrier hopping; the mobility is small ($\sim 5\times10^{-5}$ cm^2/V sec) and activated ($\Delta E=0.3$ eV). The semiconductor to metal transition is evident in the data

(OVER)

DD FORM 1 JAN 73 1473 EDITION OF 1 NOV 65 IS OBSOLETE S/N 0102-014-6601

Unclassified

SECURITY CLASSIFICATION OF THIS PAGE (When Data Entered)

20. and leads to a qualitative change in temperature dependence of the conductivity and to finite zero temparture values above $y_c \simeq 0.01-0.02$. The transport mobility increases by five to six orders of magnitude on going through the transitional region. In the metallic state, the high mobility (~60 cm^2/V sec, assuming unit charge transfer) provides evidence of the validity of a band theory approach with delocalized states in this disordered polymer. The transport in the metallic state is described as metallic strands separated by thin potential barriers. The main effect of orientation appears to be to alter the barriers. In particular, use of oriented cis-$(CH)_x$ starting material leads to significant improvement in conductivity due to smaller barrier widths and lower barrier heights. Analysis of the temperature dependence of the conductivity within this model leads to an estimate of the intrinsic conductivity in heavily doped metallic $[CH(AsF_5)_4]_x$, $\sigma \simeq 4 \times 10^4$ $ohm^{-1}cm^{-1}$ at room temperature.

OFFICE OF NAVAL RESEARCH

Contract N00014-75-C-0962

Task No. 356-602

Technical Report No. 80-4

Electrical Transport in Doped Polyacetylene

by

Y.W. Park, A.J. Heeger, M.A. Druy*
and A.G. MacDiarmid*

To be published

in

J. Chem. Phys.

Departments of Physics and Chemistry*
University of Pennsylvania
Philadelphia, Pa. 19104

July 8, 1980

ELECTRICAL TRANSPORT IN DOPED POLYACETYLENE*

Y.-W. Park and A. J. Heeger
Department of Physics
and
Laboratory for Research on the Structure of Matter

and

M. A. Druy and A. G. MacDiarmid
Department of Chemistry
and
Laboratory for Research on the Structure of Matter
University of Pennsylvania
Philadelphia, Pennsylvania 19104

Abstract

The results of an experimental study of electrical conductivity and thermopower in doped polyacetylene are reported. Included are measurements on both as-grown and partially oriented films doped with iodine and AsF_5; $\left[CH(AsF_5)_y\right]_x$ and $\left[CH(I_3)_y\right]_x$ where y covers the full doping range. The data indicate three important concentration regimes; the dilute limit ($y < 0.001$), the transitional region ($0.001 < y < 0.01$), and the metallic state ($y > 0.01$). In the dilute limit, the transport is via carrier hopping; the mobility is small ($\sim 5 \times 10^{-5}$ cm^2/V-sec) and activated ($\Delta\epsilon = 0.3$ eV). This localized state hopping is consistent with the proposed soliton doping mechanism. The semiconductor to metal transition is evident in the data and leads to a qualitative change in

---

* Work supported by the Office of Naval Research and the University of Pennsylvania Materials Research Laboratory (NSF-DMR 76-80994).

temperature dependence of the conductivity and to finite zero temperature values above $y_c \simeq 0.01 - 0.02$. The transport mobility increases by five to six orders of magnitude on going through the transitional region. In the metallic state, the high mobility (~ 60 cm^2/V-sec, assuming unit charge transfer) provides evidence of the validity of a band theory approach with delocalized states in this disordered polymer. The transport in the metallic state is described as metallic strands separated by thin potential barriers. The main effect of orientation appears to be to alter the barriers. In particular, use of oriented cis-$(CH)_x$ starting material leads to significant improvement in conductivity due to smaller barrier widths and lower barrier heights. Analysis of the temperature dependence of the conductivity within this model leads to an estimate of the intrinsic conductivity in heavily doped metallic $[CH(AsF_5)_y]_x$, $\sigma \simeq 4 \times 10^4$ Ω^{-1}-cm^{-1} at room temperature.

I. INTRODUCTION

Linear polyacetylene, $(CH)_x$, is the simplest conjugated organic polymer and is therefore of special fundamental importance. Interest in this semiconducting polymer has been stimulated by the successful demonstration of doping with associated control of electrical properties over a wide range; the electrical conductivity of films of $(CH)_x$ can be varied over 12 orders of magnitude from that of an insulator ($\sigma \sim 10^{-9}\,\Omega^{-1}\,cm^{-1}$) through semiconductor to a metal ($\sigma \sim 10^{3}\,\Omega^{-1}\,cm^{-1}$).[1,2] Various electron donating or accepting molecules can be used to yield n-type or p-type material, and compensation and junction formation have been demonstrated.[3,4] Optical-absorption studies[5,6] indicate a semiconductor with peak absorption coefficient of about 3×10^{5} cm^{-1} at 1.9 eV. Partial orientation of the polymer fibrils by stretch elongation of the $(CH)_x$ films results in anisotropic electrical[7] and optical properties[6] suggestive of a highly anisotropic band structure.[8] The electrical conductivity of partially oriented metallic $[CH(AsF_5)_{0.1}]_x$ is in excess of 2000 $\Omega^{-1}\,cm^{-1}$.

The qualitative change in electrical and optical properties at dopant concentrations above a few percent have been interpreted[2] as a semiconductor-metal transition by analogy to that observed in studies of heavily doped silicon. However, the anomalously small Curie-law susceptibility components in the lightly doped semiconductor regime[9] suggest that the localized states induced by doping below the semiconductor-metal transition are nonmagnetic. These observations coupled with electron

spin resonance studies[10,11] of neutral defects in the undoped polymer have resulted in the concept of soliton doping[12,13]; i.e. localized domain-wall-like charged donor-acceptor states induced through charge transfer doping.

The initial results obtained on conducting polymers have generated interest from the point of view of potentially low cost solar energy conversion. Experiments utilizing polyacetylene, $(CH)_x$, successfully demonstrated rectifying junction formation.[3,4,14] In particular a p-$(CH)_x$:n-ZnS heterojunction solar cell has been fabricated with open circuit photovoltage of 0.8 Volts.[4] In related experiments, a photoelectrochemical photovoltaic cell was fabricated using $(CH)_x$ as the active photoelectrode.[15]

In this paper we present the results of a detailed experimental study of the electrical transport, conductivity (σ) and thermoelectric power (S), in $(CH)_x$ doped with AsF_5 and iodine. The experimental results cover the full concentration (y) range from undoped to metallic on both partially oriented and as-grown films. The experimental techniques, including sample preparation, doping and measurement of $\sigma(T,y)$ and $S(T,y)$, are described in Section II. The results are presented in Section III and analyzed in Section IV in terms of transport in the three concentration regimes: metallic, semiconductor-metal (SM) transition, and lightly doped semiconductor. A summary and conclusion are given in Section V.

II. EXPERIMENTAL TECHNIQUES

a) Samples

Crystalline films of polyacetylene were grown in the presence of a Ziegler catalyst using techniques similar to those developed by Shirakawa et al.[16-20] X-ray diffraction and scanning electron micrograph studies show that the as-grown films, both cis and trans, are polycrystalline and consist of matted fibrils which are typically 200 Å in diameter.[16-20] Recent electron microscopy studies[22] of thin $(CH)_x$ films polymerized directly on an electron-microscope grid have shown that the fibrillar structure is the nascent morphology.[16-20,21] The measured density of the as-grown film is ca. 0.4 gm/cm^3 compared with 1.2 gm/cm^3 as obtained by flotation techniques, indicating that the volume filling fraction, f, of fibrils is approximately 1/3.

The cis-trans content was controlled by thermal isomerization.[15-19] Samples used in these studies were films (typical thickness ~ 0.1 mm) taken from the side wall of the reactor. All measurements were carried out on either ~90% cis (synthesized at -78° C) or 95% ~ 98% trans (after thermal isomerization for 2 hrs at 200° C). The cis-trans content was monitored by examination of infrared spectra.[16-20] Care was taken to achieve pure $(CH)_x$ starting material through extensive washing to remove all catalyst, with subsequent storage and handling either in vacuum or in inert atmosphere to minimize oxygen content. Chemical analysis of typical cis and trans $(CH)_x$ indicate analytical purity.*

---

* Films used had elemental analyses in the range:
C = 90.91%, H = 7.91% (total 98.82%) to
C = 91.80%, H = 7.99% (total 99.79%);
calculated values for $(CH)_x$: C 92.26%; H 7.74%.

Partially aligned films were obtained by mechanical stretching.[21,23] It was found that when cis-films of polyacetylene were extended in an inert (argon) atmosphere, ultimate extension ratios as high as 3.3 were obtained; subsequent thermal isomerization under stress resulted in $\ell/\ell_o \sim 4$ where ℓ_o and ℓ are the initial and final lengths of the film. Oriented films used in this study had $\ell/\ell_o \sim 3$. Details on the stretch orientation and the tensile properties of $(CH)_x$ are reported elsewhere.[21]

b) Doping

Doping was carried out by exposing the $(CH)_x$ films to vapor of iodine or AsF_5.[1-4,24] In the case of the iodine doping, the vapor was carried by a flow of dry N_2 gas; the dry nitrogen was first passed through a vessel containing iodine crystals at room temperature and then the gas was flowed over the $(CH)_x$ films to be doped. Doping rates could be varied by controlling the temperature (and vapor pressure) of the iodine as well as controlling the flow rate (typically 0.1 cubic feet per hour). Slow, controlled doping with AsF_5 was achieved by cooling the AsF_5 with a slush bath to ca. -100° C to reduce its vapor pressure. The AsF_5 doping was carried out in stages. In the initial stage, the sample was exposed to ≤ 0.5 torr of AsF_5. This pressure was subsequently increased in stages. The final pressure used was dependent on the desired dopant concentration; for heavily doped metallic $[CH(AsF_5)_y]_x$, $y \sim 0.1$, the final pressure was approximately 5 torr.

Specific concentrations were achieved by monitoring the conductivity of the sample (or a reference sample in the container) and comparing it with the previously calibrated curve of conductivity (room temperature) vs. concentration. The doping process was stopped when the conductivity reached the desired value. The dopant concentration was determined by weight uptake; concentrations have previously been verified by chemical analysis.[1] Samples were pumped for about 1-2 hrs under dynamic vacuum after doping, with no observable change in conductivity.

The uniformity of the doping on the microscopic scale has been studied by a variety of techniques. In the case of iodine, X-ray studies,[25] variation of the proton nuclear magnetic resonance (nmr) second moment,[26] and photoemission results[27] are consistent and imply essentially uniform doping throughout the polymer fibrils. For AsF_5, photoemission results[28] imply non-uniformity at high concentrations with a higher concentration near the surface of the fibrils. At AsF_5 concentrations below 1%, the photoemission data[28] indicate penetration of the dopant into the bulk of the fibrils.

In general, doping the cis isomer appears to give consistently higher conductivity values (about two to five times greater) than the trans isomer even though the trans isomer has a higher room temperature conductivity ($\sim 2 \times 10^{-8} \Omega^{-1} cm^{-1}$) than the cis-isomer ($\sim 2 \times 10^{-9} \Omega^{-1}\text{-}cm^{-1}$). Optical absorption,[29] thermopower,[30] and nmr 2nd moment[26] studies indicate

that cis-trans isomerization takes place during iodine doping. Thus, the same final product is obtained from both isomers when they are heavily doped, and that product is primarily trans-$(CH)_x$. It is not yet clear to what extent AsF_5 doping induces similar isomerization. The higher conductivities obtained with cis starting material suggest that the doping induced isomerization leads to higher quality trans material than thermal isomerization with subsequent doping.

c) Electrical Conductivity Measurements

All conductivity measurements utilized four-probe techniques. The values given were obtained directly from the measured resistance and the measured sample dimensions. No corrections have been made for the low density associated with the fibrillar structure of the $(CH)_x$ films.

Due to the chemical activity of iodine and AsF_5, the sample holders were made with glass frames and utilized platinum leads; Electrodag was used to make the electrical contacts onto the polymer samples. Typically, the contacts were applied in air with exposure time kept to a minimum; the mounted samples were pumped in vacuum for 2-3 hours until the contacts were dry. The effect of the solvent in the Electrodag paint was checked by applying the contacts before and after doping. The metallic conductivity of samples mounted before doping was typically 50% higher than that of the samples whose contacts were applied after the samples were doped. In addition to Electrodag, gold evaporated contacts and mechanical (pressed) contacts have been tried. The various contacts yield conductivity data

which are consistent and without significant differences. The effects of different contacts have also been studied by Kwak et al.[31] The conductivity data presented in this paper were obtained from samples mounted before doping, unless otherwise stated. Contacts were checked to be ohmic for currents from 10^{-10} - 10^{-5} amps for undoped $(CH)_x$, and from 10^{-6} - 10^{-2} amps for metallic samples.

To check the effect of the air exposure on the undoped $(CH)_x$, an on-line experiment was set up to monitor conductivity vs. time. Samples were mounted in a glove bag under argon atmosphere. In the first three hours of air exposure, the conductivity of cis-$(CH)_x$ increased by one order of magnitude while that of trans-$(CH)_x$ increased by only about a factor of three. Upon pumping out the air, the conductivity returned to its initial value. Such reversibility was also observed earlier in electron spin resonance experiments.[10] Air exposure of heavily doped metallic samples for 2 hours resulted in a 40% and 20% decrease, respectively, for $[CH(AsF_5)_y]_x$ and $[CH(I_3)_y]_x$. Studies of the effect of oxygen on metallic $[CH(I_3)_y]_x$ samples showed a decrease in conductivity of about 10% in the first four hours.

In an initial attempt to stabilize the samples after doping, paraffin wax coatings were applied. Conductivity measurements of uncoated and wax coated metallic $[CH(I_3)_y]_x$ were carried out on samples doped at the same time and under identical conditions. The conductivity of the wax coated sample decreased only 10% after 12 hours, whereas the conductivity of the uncoated sample fell by a factor of five during the same period.

Similar tests were carried out in connection with the temperature dependence measurements. The temperature dependence exhibited by doped samples obtained from the bottom of the reactor was not significantly different from that obtained from samples extracted from the side walls. Using cis samples of either origin, metallic AsF_5-doped $(CH)_x$ showed a slight increase in conductivity (a few per cent) below room temperature as noted previously.[32] Samples mounted after doping, or samples re-painted with solvent containing Electrodag, showed a monotonic decrease in conductivity with decreasing temperature. Exposure to air had similar effects; the weak maximum reduced in magnitude and shifted toward higher temperature before disappearing after ~ 30 minutes exposure. The wax coated samples showed similar temperature dependences to those of the uncoated ones.

d) Thermopower Measurements

A rectangular sample (3mm x 25mm) was cut from the polymer film and mounted lengthwise between two copper blocks using pressure contacts. The temperature difference (ΔT) was established by heating one of the copper blocks and the voltage (generated by the thermal gradient across the sample) was measured. Typically $\Delta T \sim 2K$ was used during each measurement, so that the thermopower is an average over this interval. The measurement of ΔT across the sample utilized a copper-constantan differential thermocouple. The thermodynamically stable

trans-$(CH)_x$ was used in all the thermopower measurements. The iodine and AsF_5 concentrations in the doped samples were determined as described above. Reproducibility for independently prepared samples was about ± 10% at the lightest doping levels and better than ± 5% in the metallic regime. Due to the extremely rapid increase of the conductivity at low dopant levels, the uncertainty in y was ± 0.001 for concentrations below y = 0.01 (1 mole %). Even at the highest dopant levels, the accuracy in y was always better than ± 0.005.

III. EXPERIMENTAL RESULTS

a) Thermopower

The room temperature results, S vs log y for trans-$[CH(I_3)_y]_x$ are shown in Fig. 1. The sign of S is positive throughout the entire concentration range indicating p-type behavior consistent with charge transfer doping to the iodine acceptor and the formation of I_3^-. The semiconductor-metal transition is clearly evident in Fig. 1. Note that S is relatively insensitive to the dopant concentration up to approximately y = 0.001. For the undoped trans-$(CH)_x$, S = (900 ± 50) μV/K and then decreases slightly to S = (750 ± 50) μV/K at y = 0.001. Figure 1 shows the earlier data[30] in more detail with additional points in the transitional region. As shown in our previous paper,[30] within the measurement accuracy, the thermopower is independent of temperature in the lightly doped regime ($y \leq 0.001$). At concentrations above the SM transition, S decreases with decreasing temperature.[30]

The thermopower in the metallic limit is shown in Fig. 2, including the results for both unoriented cis-$[CH(AsF_5)_{.147}]_x$ and partially oriented trans-$[CH(AsF_5)_{.096}]_x$ with $\ell/\ell_o = 3.2$. Any variation between oriented and unoriented samples is comparable to the variations observed from sample to sample (indicated by error bars on Fig. 2). No qualitative difference and no significant anisotropy are observed; S(T) is essentially the same for oriented and as-grown samples. This is consistent with expectations. Since thermoelectric power is a zero-current transport coefficient, interfibril contacts should be unimportant allowing an evaluation of the intrinsic metallic properties. The magnitude and temperature dependence of S (Fig. 2) are characteristic of a degenerate electron gas and are indicative of intrinsic metallic behavior.[30,31]

For dilute concentrations well below the semiconductor-metal transition the thermopower is large and essentially temperature independent. Such behavior can be understood for a dilute concentration of carriers (holes) which hop among a set of localized states. In this case, where the kinetic energy of the carriers is negligible, the thermopower is given by the Heikes formula[33,34]

$$S = +\frac{k_B}{|e|} \ell n[(1-\rho/\rho] \qquad (1)$$

where $\rho = n/N$ is the ratio of the number of holes (n) to the number of available sites (N) (eq. 1 assumes spinless carriers; the inclusion of spin degeneracy[34] changes the expression to $S = +(k_B/|e|)\ell n(2-\rho)/\rho)$. Identification

with the experimental data for undoped trans-$(CH)_x$ requires that $\rho \simeq 10^{-4}$ and temperature independent. This value corresponds to a carrier concentration of 2×10^{18} cm^{-3} in "undoped" $(CH)_x$ and is consistent with the results of capacitance vs voltage studies[35] of p-$(CH)_x$: n-CdS heterojunctions using CdS with known carrier concentration. The results therefore imply that in the undoped polymer, the conductivity is due to a small number of residual carriers ($\rho_o \simeq 10^{-4}$) provided by defects and/or impurities, and that the mobility results from hopping. The insensitivity of the thermopower to iodine concentrations less than 0.1 mole% (or 0.1% I_3^-) is consistent with this interpretation and implies that ρ_o is well below 10^{-3}. From eq. 1, the thermopower at $y = 10^{-3}$ should be 0.75 of that at $y = 10^{-4}$; consistent with Fig. 1 to within the combined uncertainty in y and ρ.

b) Conductivity

By careful control of the dopant concentration, any specified conductivity can be obtained covering the range from $\sigma = 2 \times 10^{-9}$ Ω^{-1}-cm^{-1} to $\sigma > 10^3$ Ω^{-1}-cm^{-1} using cis-$(CH)_x$ starting material. Higher metallic values, $\sigma > 3000$ Ω^{-1}-cm^{-1}, were obtained using cis starting material, stretch-oriented ($\ell/\ell_o = 3.1$) and then doped with AsF_5. Since exposure of undoped $(CH)_x$ to ammonia vapor[2] decreases σ to values below 10^{-10} Ω^{-1}-cm^{-1}, the accessible range covers more than thirteen orders of magnitude.

The temperature dependences of AsF_5-doped $(CH)_x$, both as-grown, and stretch-oriented are shown in Fig. 3, for a variety of dopant concentrations. The temperature range covered by the measurements depended on the resistance of the sample; for the highest conductivity sample, data were obtained over the entire range from 300 to 1.8 K. The curvature

seen in log σ vs 1/T was noted earlier for halogen dopants.[35] This curvature may arise from disorder, for example, leading to a distribution of activation energies. Alternatively variable range hopping[36] may play a role at low temperatures. Taking the initial slope of the log σ vs 1/T plots, we obtain the activation energy, ΔE, which serves as a simple index of the conductivity behavior. The results are presented in Fig. 4 where data from AsF_5-doped samples and iodine doped samples are plotted versus concentration on a logarithmic scale. Note that the iodine doped samples are formulated as $[CH(I_3)_y]_x$ since the I_3^- ion is known to be present.[37] Using this formulation the data from the two dopants are in good agreement, although the AsF_5 doped samples give consistently lower activation energies above y = 0.01 consistent with the higher metallic conductivity. The activation energy of the undoped trans-$(CH)_x$ is ΔE = (.3 ± .03) eV. ΔE is relatively insensitive to the dopant concentration up to y = 0.001, and then decreases rapidly through the SM transition. Above y = 0.01 (1 mole %) ΔE is small and nearly independent of the concentration; the conductivity is no longer activated in heavily doped $(CH)_x$.

The room temperature values from Fig. 3 are replotted as σ vs y in Fig. 5. The value $y = 10^{-4}$ for undoped $(CH)_x$ was determined from the magnitude of the thermopower, as described above;[34] the point at y = 0.003 was determined by weight uptake. In the dilute concentration regime, σ increases approximately in proportion to the dopant concentration, so that

the mobility is independent of y. Note that in this dilute regime, the activation energy (Fig. 4) is also insensitive to the dopant concentration. Figures 4 and 5, together with the temperature independence of the thermopower,[30] imply that in the dilute regime the transport is via carrier hopping; the conductivity results from a temperature independent carrier concentration (proportional to y) and an activated mobility.[38]

The temperature dependence of the conductivity in the metallic high concentration limit is shown more clearly in Figure 6, where σ/σ_{RT} vs. T is plotted in a linear scale. The room temperature conductivity values for these partially oriented films were measured independently by simple four-probe and by Montgomery[39] techniques. The results, compared in Table 1, are in general agreement. For heavily doped metallic $[CH(AsF_5)_{0.14}]_x$ (oriented with $\ell/\ell_o = 3.1$), the conductivity first increases on cooling below room temperature,[7,31] goes through at maximum at 220 K, then decreases and becomes constant below 5 K with $\sigma(0)/\sigma(300\ K) = 0.66$. The conductivity maximum near room temperature varies from sample to sample, but in general cis-$(CH)_x$ starting material leads to a larger maximum than trans-$(CH)_x$. Also shown in Fig. 6 are the results for $[CH(I_3)_{.08}]_x$ ($\ell/\ell_o = 3.1$). The conductivity decreases monotonically and appears to be going to zero as $T \rightarrow 0$. The low temperature data from these samples are shown in more detail in Fig. 7 where we plot the normalized conductivity (log scale) vs 1/T. For the metallic $[CH(AsF_5)_{0.14}]_x$, the conductivity at low temperatures approaches the constant value,[31]

$\sigma(0) \simeq 800\ \Omega^{-1}\text{-cm}^{-1}$. For the iodine doped $[CH(I_3)_{0.08}]_x$, the low temperature conductivity continues to be activated, even though the room temperature value is comparable to that of the AsF_5 doped sample.

Considering the matted fibril structure of polyacetylene the temperature independence of the conductivity (see Fig. 7) suggests a tunneling mechanism through the interfibril contact barriers in addition to the thermally activated charge transfer over the barriers located between large metallic conducting fibers. The residual activation for heavily doped $[CH(I_3)_y]_x$ is not understood. However, this may indicate that even the heavily iodine doped samples are only just on the verge of metallic behavior.

The temperature dependence of the conductivity of <u>trans</u>-$[CH(AsF_5)_{0.10}]_x$ samples, both partially oriented with elongation ratio $\ell/\ell_0 = 2.8$ and unoriented, are shown in Fig. 8. The two samples were prepared from the same starting material and were doped simultaneously. The temperature dependences of the normalized conductivities are similar although the room temperature values varied considerably (for $\ell/\ell_0 = 2.8$, $\sigma_{\parallel} = 1400\ \Omega^{-1}\text{-cm}^{-1}$ and $\sigma_{\perp} = 280\ \Omega^{-1}\text{-cm}^{-1}$; for $\ell/\ell_0 = 1$, $\sigma_{\parallel} = \sigma_{\perp} = 240\ \Omega^{-1}\text{-cm}^{-1}$). Furthermore, at low temperatures all four samples approach nearly temperature independent behavior as shown in Fig. 9. The low temperature normalized values are somewhat higher in the oriented samples. These results indicate that the role of the interfibril contact barriers are similar in each direction, and that the barrier height and/or widths are slightly

smaller for the partially oriented films. The temperature dependence of σ for a partially oriented film ($\ell/\ell_o \sim 3$) which has been exposed to the air during the isomerization under stress, flattens more slowly resulting in $\sigma(1.8\ K)/\sigma(300\ K) = 10^{-2}$. Combined with the observation of decreasing tensile strength after air exposure, this result suggests that the cross linking induced by the air exposure makes the interfibril contact barriers effectively larger.

Although the temperature dependences of the normalized conductivities are the same, the room temperature conductivity in the parallel and transverse direction of the partially aligned films are different about factor of five for the $\ell/\ell_o = 2.8$ sample of Figs. 8 and 9. Since the interfibril contact barriers are same in either direction, the large difference in absolute magnitude is evidently due primarily to the difference in total number of chains in the respective directions. Since the films are not perfectly oriented, there are chains going along the transverse direction in the partially oriented films. Thus, more complete orientation can be expected to yield larger values for $\sigma_{||}$ and for the anisotropy $\sigma_{||}/\sigma_{\perp}$. In this context, the thermopower data of Fig. 2 are readily understood. Even in the transverse direction $\sigma_{||}$ dominates the transport so that S is determined by $S_{||}$.[40] Determination of $S_{\perp}$ will require nearly complete orientation.

The temperature dependences of the normalized conductivity of <u>trans</u>-$[CH(AsF_5)_y]_x$ films are shown in Fig. 10 with values of y spanning the SM transition. The films were partially oriented to minimize interfibril

contact effects. A qualitative change in behavior is observed at the SM transition ($y = y_c$). At low concentrations the curves appear thermally activated and $\sigma \to 0$ as $T \to 0$. Above y_c, the curvature changes and the conductivity remains finite as $T \to 0$. The low temperature normalized conductivity appears to be an excellent indicator of the SM transition in AsF_5 doped $(CH)_x$ as shown in Fig. 11. From Fig. 11 we infer $y_c \simeq 0.01\text{-}0.02$. Note that, as described above, for the iodine doped samples it appears that $\sigma \to 0$ as $T \to 0$ even at the highest doping levels. Thus, either the interfibril barrier effects are significantly more important or the metallic state is not truly achieved even at the highest doping levels.

IV. DISCUSSION

a) Semiconductor-Metal Transition; Mobility

The transition from semiconductor to metal is most clearly evident in the normalized conductivity data of Figs. 10 and 11 obtained from partially oriented films. The qualitative change in temperature dependence and finite zero temperature values above $y_c \simeq 0.01\text{-}0.02$ are indicative of an abrupt change in behavior as a function of dopant concentration. For iodine doping the situation is somewhat less clear as noted by others[41] and described in Section IIIb.

We note that the critical concentration, y_c, for the SM transition, as inferred from the conductivity data of Figs. 10 and 11, appears to be somewhat below that inferred from the onset of Pauli susceptibility;[9] from

the conductivity data we infer $0.01 < y_c < 0.02$, whereas the susceptibility data suggest $y_c > 0.02$. Additional susceptibility studies are underway to provide a more detailed and accurate description of the transitional regime.

Direct measurements of the mobility (e.g. time of flight, etc.) are not available. Although Hall effect data have been reported in the metallic regime,[42] the Hall coefficient is two orders of magnitude below that expected on the basis of approximately one carrier per dopant and may be dominated by the fibril structure of the composite medium. Some important information on the transport mobility in the semiconductor and metallic limits can be obtained directly from the conductivity.

In lightly doped <u>trans</u>-$(CH)_x$, the mobility is activated as described in Section IIIb with a room temperature value of $\mu \equiv \sigma/ne \simeq 5 \times 10^{-5}$ cm^2/V-secs (see Fig. 12). For $y > 0.003$, one finds a dramatic increase in μ. At higher dopant levels (i.e. in the transitional regime) ΔE is changing so that it is not possible to extract μ from the conductivity.

In the metallic regime, e.g. $[CH(AsF_5)_{0.1}]_x$ the number of carriers can be estimated by assuming unit charge transfer per dopant or from the oscillator strength as obtained from optical studies.[29] The latter results suggest that in the heavily doped metallic state <u>all</u> the π-electrons contribute to the metallic transport; thus $n(\text{metal}) \simeq 2 \times 10^{22}$ cm^{-1}. Taking the intrinsic conductivity to be $\sigma^{dc}_{intrinsic} \geq 2 \times 10^4\ \Omega^{-1}\text{-cm}^{-1}$ as inferred from analysis

of the optical data,[29] one obtains $\mu(\text{metal}) \geq 6\ cm^2/V\text{-sec}$. Note that assuming that all π-electrons contribute requires that heavy doping removes the bond-alternation leading to a uniform bond length polyene. Taking the somewhat more conservative point of view of one carrier per dopant, the corresponding value for $[CH(AsF_5)_{0.1}]_x$ would be $n \sim 2 \times 10^{21}$ with $\mu \geq 60\ cm^2/V\text{-sec}$. This latter value is plotted in Fig. 12 as characteristic of the metallic state.

Although there is considerable uncertainty in the absolute values in both limits, the results nevertheless demonstrate a remarkable change in mobility, five or six orders of magnitude, on going through the transitional region. This large increase in μ represents perhaps the clearest indication of a major change in electronic structure and/or transport mechanism at the SM transition in doped polyacetylene.

b) Metallic State

The high mobility in the metallic state is unexpected in view of the extensive disorder; the doped polymer is only partially crystalline and contains $\sim 10\%$ charged impurities in random interchain positions. Given the considerable evidence of one-dimensionality from transport,[7] optical[6,29] and nmr studies,[43] the effects of disorder would be expected[44] to be particularly large.

The thermopower data in the high concentration limit provide independent information on the metallic state and are consistent with

metallic behavior.[30,31] For a nearly filled band (i. e. p-type) metallic system, the thermopower can be written as

$$S = +\frac{\pi^2}{3}\left(\frac{k_B}{|e|}\right) kT \left[\frac{d\ell n\sigma(E)}{dE}\right]_{E_F} \qquad (2)$$

where $\sigma(E) = n(E)|e|\mu(E)$ and $n(E)$ is the number of carriers contributing to $\sigma(E)$, $dn(E)/dE = g(E)$ is the density of states (both signs of spin) and $\mu(E)$ is the energy dependent mobility. Assuming energy independent scattering ($\mu(E)$ independent of E)

$$S = +\left(\frac{k_B}{|e|}\right)\frac{\pi^2}{3} k_B T\, \eta(E_F) \qquad (3)$$

where $\eta(E_F) = g(E_F)/N$ is the density of states per carrier. As indicated in Fig. 2 and in earlier papers,[30,31] S is a linear function of T for AsF_5-doped metallic $(CH)_x$ whereas for heavy iodine doping there is curvature in S vs T. Nevertheless, in both cases, the thermopower decreases smoothly toward zero as $T \to 0$ in a manner typical of metallic behavior even at temperatures as low as 2 K. The experimental results (Fig. 2) are in good agreement with eq. 3 with $\eta(E_F) = 1.36$ states per eV per carrier. Since there are 0.15 carriers per carbon atom in $[CH(AsF_5)_{0.15}]_x$ (assuming complete charge transfer), the thermopower data yield for the density of states, $g(E_F) \simeq 0.2$ states per eV per C atom in good agreement with the value obtained from magnetic susceptibility measurements.[9]

Although the conductivity is weakly activated below 50 K and becomes temperature independent at low temperatures, the thermopower data imply intrinsic metallic behavior at all temperatures. We therefore conclude that the dc transport is limited by interfibril contacts, and that the heavily doped polymer can be described as consisting of metallic strands separated by thin potential barriers. This is consistent with optical studies[29] which indicate that the intrinsic individual strand conductivity is much higher than the dc value.

A model appropriate to a composite medium consisting of metallic particles dispersed at high density in an insulating matrix was recently developed by Sheng et al.[45] Fluctuation induced tunneling through potential barriers leads to the bulk dc conductivity at low temperatures with activation over the barriers at higher temperatures. We identify the conducting aggregates of Sheng et al.[45] with the metallic fibrils and assume that the barriers are due to interfibril contacts. Sheng et al.[45] assume a parabolic barrier, $V = V_o - (4V_o/W)x^2$, where V_o and W are the barrier height and thickness, respectively. We assume the cross sectional area, A, of the barriers is typically equal to that of the polymer fibrils whose diameter is ~ 200 Å. In terms of these parameters, the conductivity (σ_j) of the junction can be expressed as

$$\sigma_j(T) = \sigma_o e^{-\frac{T_1}{T + T_o}} \qquad (4)$$

where

$$T_1 = \frac{2AV_o^2}{\pi e^2 k_B W} \qquad (5)$$

and

$$T_o = \frac{4\hbar A V_o^{3/2}}{\pi^2 e^2 k_B (2m)^{\frac{1}{2}} W^2} \qquad (6)$$

The parameters T_1 and T_o are obtained experimentally from the slope and intercept, respectively, of plots of $[\ln(\sigma/\sigma_{RT})]^{-1}$ vs T as shown in Fig. 13. The results are summarized in Table 2. Typical values for T_1 and T_o are comparable and lead to barrier thickness of 10 - 20 Å and barrier heights of order $3 - 7 \times 10^{-3}$ eV. The main effect of orientation appears to be the alteration of the barrier parameters. For example, doping with oriented cis-$(CH)_x$ starting material significantly reduces both the barrier thickness and the barrier height. With this model, the dc conductivity in the metallic state can be viewed as resulting from resistors in series. The metallic strands are in series with the junctions, so that $R_{dc} = R_i(T) + R_j(T)$ where $R_i(T)$ results from the doped metallic strands with an intrinsic metallic conductivity, and R_j is the junction resistance. Assuming $R_i(T) = aT$ (near room temperature) and $R_j = R_o \exp[T_1/T + T_o]$, the magnitude of the conductivity maximum in the data of Figs. 6 and 10 implies that $R_i/R_j < 10^{-1}$ at room temperature. We thereby obtain an estimate of the intrinsic conductivity in heavily doped metallic $[CH(AsF_5)_y]_x$, $\sigma(300\ K) \simeq 4 \times 10^4\ \Omega^{-1}\text{-cm}^{-1}$.

c) Light Doping, $y < 0.001$

In this low concentration regime, the number of carriers is proportional to the concentration of dopants, and the activation energy remains constant. Moreover, the temperature independent thermopower indicates a temperature independent carrier concentration implying that the mobility is activated. We therefore conclude that in the dilute regime

$$\sigma = ne\mu \tag{7}$$

where n is the number of carriers (equal to the number of dopants) and the mobility is given by

$$\mu = \mu_o e^{-\Delta E/kT} \tag{8}$$

with $\Delta E = 0.3$ eV as indicated on Fig. 4. Such a small, thermally activated mobility is unexpected in a broad bandwidth semiconductor like $(CH)_x$. Although one might suggest that the activated transport is limited by disorder in the polymer, the high conductivity and high mobility in the metallic state argue to the contrary. One might argue that the observed activation energy is the result of int··ibril contact resistance. However, the activation energy is ins· .tive to whether the polymer is taken as-grown or stretch-oriented. (Note that the low temperature results in the metallic regime show major changes in interfibrillar contact effects on orientation; see Figs. 7, 8, and 9). Moreover, nearly identical results are obtained

from low density foam-like material synthesized using a gel as an intermediate step; whereas the fibril density is down by more than an order of magnitude, and the fibril diameter is three to five times larger.[46]

The localized state hopping transport inferred from the thermopower measurements below y = 0.001 is qualitatively consistent with the proposed[9,30,47] soliton doping mechanism. Motion of the charged localized domain-walls would be expected to be via diffusive hopping in agreement with the low mobility inferred from Fig. 5 for y < 0.001. Moreover, for a fixed impurity concentration the number of charged kinks would be independent of temperature in agreement with the temperature independent thermopower found in the dilute limit. Finally, although the domain-wall would be distributed over a group of carbon atoms, the center of mass of the wall could take any position along the chain so that the number of available sites would be of order the number of carbon atoms in agreement with the magnitude of the thermopower.

The formation of domain-walls, or solitons on long chain polyenes has been studied theoretically by Rice[12] and by Su, Schrieffer and Heeger.[13] The electronic structure of the soliton exhibits a localized state φ_0 at the center of the gap, containing one electron for the neutral kink. While this localized state is spin unpaired, the distorted valence band continues to have spin zero. Thus, the neutral soliton has spin 1/2. The static susceptibility therefore will contain a Curie law contribution and can be used to count the number of neutral soliton defects present. Spin

resonance linewidth[11] and nmr relaxation[43] studies have demonstrated mobile spin species spread out over many lattice constants in agreement with these ideas. The number of unpaired spins, typically one per 3000 carbon atoms is comparable to the number of charge carriers in the undoped polymer (~ one per 10,000 carbon atoms) inferred from the thermopower.

Since the localized state occurs at the gap center, i.e. the chemical potential, the relevance of the solitons to the doping of $(CH)_x$ depends on the energy for creation of a soliton, E_s, as compared with the energy required for making an electron or a hole, $\frac{1}{2}Eg = \Delta$. Numerical estimates[13] indicate that soliton formation is energetically favorable, i.e. $E_s < \Delta$. Moreover, Takayama et al.[48] have recently developed a continuum model in which they find $E_s = \frac{2}{\pi}\Delta$; i.e. always less than Δ.

From these observations we suggest that in the undoped <u>trans</u>-$(CH)_x$, a fraction of the isomerization induced defects has been ionized by residual impurities to give the observed density ($\rho \sim 10^{-4}$). Subsequent doping will ionize more and/or create additional charged kinks.

In the case of diffusive hopping, the mobility is given by the Einstein relation, $\mu = eD/kT$, where D is the diffusion constant. To obtain an estimate of the diffusion constant we use the result of Wada and Schrieffer[49] (WS) for one-dimensional Brownian motion of domain-walls in contact with thermal phonons

$$D_{WS} = 0.516\, \omega_o a^2 \left(\frac{k_B T}{M \omega_o^2 u_o^2}\right)^2 \qquad (9)$$

where M is the atomic (C-H) mass, u_o is the equilibrium amplitude of the distortion and ω_o is the attempt frequency. In the double-well ψ^4 theory considered by WS, ω_o is the harmonic vibration frequency for an atom near the minimum of either well. In $(CH)_x$, we may take $\omega_o^2 = K/M$ where $K = 10.5$ eV/Å^2 is the spring constant.[50] Wada and Schrieffer[49] consider the interaction between neutral, free domain-walls and phonons. At room temperature using M = 13 AMU, $a \simeq 1.4$ Å and $u_o \simeq 0.04$ Å, we find $D_{WS} \simeq 2 \times 10^{-2}$ cm^2/sec ($D_{WS}/a^2 \simeq 10^{14}$) in agreement with the measured[43] diffusion constant of the neutral magnetic solitons in undoped <u>trans</u>-$(CH)_x$.

In the case of charged solitons one might argue that the hopping attempt frequency is reduced by the Coulomb binding of the wall to the acceptor ion and assume that

$$D_{(CH)_x} = D_{WS} e^{-\Delta E/k_B T} \tag{10}$$

so that for lightly doped $(CH)_x$

$$\mu_{(CH)_x} = \frac{e}{k_B T} D_{WS} e^{-\Delta E/kT}$$

$$= 0.516 \left(\frac{e}{k_B T}\right) \omega_o a^2 \left(\frac{k_B T}{M\omega_o^2 u_o^2}\right)^2 e^{-\Delta E/k_B T} \tag{11}$$

For the charged soliton, with $\Delta E \simeq 0.3$ eV, $D_{(CH)_x} \simeq 2 \times 10^{-7}$ at room

temperature leading to a mobility of $\mu_{(CH)_x} \simeq 10^{-5}$ cm^2/V-sec. Although of the correct magnitude, such a picture would imply hopping between impurity sites whereas the data indicate that the number of available sites is much larger;[38] i.e. comparable to the number of carbon atoms per unit length on the chain. A detailed understanding of the diffusion (and mobility) of charged solitons is clearly lacking. However, we would anticipate that the activation energy for motion of a charged soliton (on an otherwise perfect chain) would be much greater than that of a neutral soliton.[13] Theoretical study of the charged soliton mobility is required for further progress.

The hopping mobility discussed above is appropriate to steady state (dark) transport in the dilute limit. However, the transport mobility appropriate to photogenerated carriers may be considerably higher. Since a soliton-like distortion would be expected to form around a photogenerated carrier only after a considerable time delay, the band mobility might be appropriate. Particularly in junctions where the carriers are rapidly swept out by the junction electric field, a mobility greater than or equal to that found in the metallic state would be expected.

V. Summary and Conclusion

The transport data presented in this paper indicate three important concentration regimes:

1) $y < 0.001$; the dilute limit where carriers introduced by doping act independently

2) $0.001 < y < 0.01$; the transitional region

3) $y > 0.01$, the metallic state.

From analysis of the data, we have been able to draw specific conclusions relevant to these three regimes.

In the dilute limit, the transport is via carrier hopping; the mobility is small ($\sim 5 \times 10^{-5}$ cm^2/V-s) and activated ($\Delta E = 0.3$ eV). This localized state hopping transport is consistent with the proposed soliton doping mechanism. Based on the soliton interpretation of the steady state (dark) transport in the dilute limit, it was argued that the mobility appropriate to photogenerated carriers may be considerably higher; i.e. greater than or equal to that found in the metallic state.

The semiconductor-metal transition is evident in $[CH(AsF_5)_y]_x$ and results in a qualitative change in temperature dependence of the conductivity and finite zero temperature values above $y_c \simeq 0.01 - 0.02$. For iodine doping the situation is somewhat less clear.

The transport mobility in $[CH(AsF_5)_y]_x$ increases dramatically on going through the transitional region. This large increase (five to six orders of magnitude) represents perhaps the clearest indication of a major change in electronic structure and/or transport mechanism at the SM transition.

The high mobility in the metallic state (~ 60 cm^2/V-sec assuming complete charge transfer with one carrier per dopant molecule) provides strong evidence of the validity of a band theory approach with delocalized states in this disordered metallic polymer. Even in this context the

mobility is surprisingly large; the inferred values are comparable to the mobilities found in the best metals (e.g. for copper $\mu \sim 50$ cm^2/V-sec at room temperature).

The metallic state is described as metallic strands separated by thin potential barriers (typically $W < 20$ Å and $V_o < 10^{-2}$ eV). Electron transfer through the barriers is via tunneling at low temperatures, with activation over the barriers at higher temperature. The main effect of orientation appears to be to alter the properties of the barriers. In particular, doping oriented cis-$(CH)_x$ starting material leads to significant improvement in conductivity due to smaller barrier widths and lower barrier heights. Analysis of the temperature dependence of the conductivity within this model leads to an estimate of the intrinsic conductivity in heavily doped metallic $[CH(AsF_5)_y]_x$, $\sigma \simeq 4 \times 10^4\ \Omega^{-1}\text{-cm}^{-1}$ at room temperature.

These and related transport results must be viewed in the context of the broad based experimental study of the chemical and physical properties of this new class of conducting polymers. The transport data provide insight into many aspects of the problem. However, detailed understanding of the doping mechanism, charge transport, electronic structure, and the semiconductor to metal transition will require combined input including, in particular, structural, optical and magnetic information.

Acknowledgement: We thank S. C. Gau and A. Pron for help in sample preparation.

TABLE 1

Comparison of four-probe and Montgomery results for $\sigma_{||}$ and $\sigma_{\perp}$ on oriented samples at room temperature.

	$\ell/\ell_o = 3.1$	4-Probe (Ω^{-1}-cm^{-1})	Montgomery (Ω^{-1}-cm^{-1})
cis-$[CH(AsF_5)_{.14}]_x$	$\sigma_{||}$	2450	2350
	$\sigma_{\perp}$	-	377
cis-$[CHI_{.25}]_x$	$\sigma_{||}$	1500	1620
	$\sigma_{\perp}$	-	203
trans-$[CH(AsF_5)_{.10}]_x$	$\sigma_{||}$	1800	2800
	$\sigma_{\perp}$	120	220

TABLE 2

Barrier parameters obtained from analysis of low temperature data obtained with metallic $[CH(AsF_5)_y]_x$

Sample	ℓ/ℓ_o		T_1	T_o	W (Å)	V_o (eV)
trans-$[CH(AsF_5)_{.10}]_x$	1.0	$\sigma_{\|\|}$	48.1	41.3	17 Å	7.2×10^{-3} (eV)
		$\sigma_\perp$	47.8	39.0	18 Å	7.5×10^{-3}
trans-$[CH(AsF_5)_{.10}]_x$	2.8	$\sigma_{\|\|}$	35.0	37.3	16 Å	5.8×10^{-3}
		$\sigma_\perp$	54.7	54.0	15 Å	7.2×10^{-3}
cis-$[CH(AsF_5)_{.14}]_x$	3.1	$\sigma_{\|\|}$	21.4	48.9	9.2 Å	3.5×10^{-3}

References:

1. Shirakawa, H., Louis, E. J., MacDiarmid, A. G., Chiang, C. K., and Heeger, A. J., Chem. Commun. 578 (1978); Chiang, C. K., Druy, M. A., Gau, S. C., Heeger, A. J., Shirakawa, H., Louis, E. J., MacDiarmid, A. G. and Park, Y. W., J. Am. Chem. Soc. 100, 1013 (1978)
2. Chiang, C. K., Fincher, C. R., Jr., Park, Y. W., Heeger, A. J., Shirakawa, H., Louis, E. J., Gau, S. C. and MacDiarmid, A. G., Phys. Rev. Lett. 39, 1098 (1977)
3. Chiang, C. K., Gau, S. C., Fincher, C. R., Jr., Park, Y. W., MacDiarmid, A. G. and Heeger, A. J., Appl. Phys. Lett. 33, 181 (1978)
4. Ozaki, M., Peebles, D., Weinberger, B. R., Chiang, C. K., Gau, S. C., Heeger, A. J. and MacDiarmid, A. G., Appl. Phys. Lett. 35, 83 (1979)
5. Shirakawa, H., Ito, T., Ikeda, S., Polym. J. 4, 460 (1973)
6. Fincher, C. R., Jr., Peebles, D. L., Heeger, A. J., Druy, M. A., Matsumura, Y., MacDiarmid, A. G., Shirakawa, H. and Ikeda, S., Solid State Commun. 27, 489 (1978)
7. Park, Y. W., Druy, M. A., Chiang, C. K., Heeger, A. J., MacDiarmid, A. G., Shirakawa, H. and Ikeda, S., Polymer Lett. 17, 195 (1979)

8. Grant, P. M. and Batra, I. P., Solid State Commun. 29, 225 (1978)

9. Weinberger, B. R., Kaufer, J., Heeger, A. J., Pron, A. and MacDiarmid, A. G., Phys. Rev. B 20, 223 (1979)

10. Goldberg, I. B., Crowe, H. R., Newman, P. R., Heeger, A. J. and MacDiarmid, A. G., J. Chem. Phys. 70, 1132 (1979)

11. Weinberger, B. R., Kaufer, J., Heeger, A. J. and MacDiarmid, A. G., Phys. Rev. Lett. (Submitted)

12. Rice, M. J., Phys. Lett. 71A, 152 (1979)

13. Su, W. P., Schrieffer, J. R. and Heeger, A. J., Phys. Rev. Lett. 42, 1698 (1979)

14. Tani, T., Gill, W. D., Clarke, T. C., and Street, G. B., Preprint, IBM Symposium on Conducting Polymers, March 29, 30, 1979

15. Chien, S. N., Heeger, A. J., Kiss, Z., MacDiarmid, A. G., Gau, S. C. and Peebles, D. L., Appl. Phys. Lett. (to be published)

16. Shirakawa, H. and Ikeda, S., Polym. J. 2, 231 (1971)

17. T. Ito, H. Shirakawa and S. Ikeda, Kobunshi Ronbunsha 5, #6 (1976) p. 470 (English edition)

18. Ito, T., Shirakawa, H. and Ikeda, S., J. Polym. Sci. Polym. Chem. Ed. 12, 11 (1974)

19. Ito, T., Shirakawa, H. and Ikeda, S., J. Polym. Sci. Polym. Chem. Ed. 13, 1943 (1975)

20. Shirakawa, H., Ito, T. and Ikeda, S., Die Macromoleculare Chemie 179, 1565 (1978)

21. Druy, M. A., Tsang, Chi-Hwa, Brown, N., Heeger, A. J. and MacDiarmid, A. G., J. Polym. Sci. Polym. Phys. Ed. (in print)

22. Karasz, F. E., Chien, J. C. W., Galkiewicz, R., Wnek, G. E., Nature (in press)

23. Shirakawa, H. and Ikeda, S., ACS-CSJ Chemical Congress, Honolulu, Hawaii, April 1-6 (1979)

24. MacDiarmid, A. G., and Heeger, A. J., Preprint, IBM Symposium on Conducting Polymers, March 29, 30 (1979)

25. Hsu, S., Signorelli, A., Pez, G. and Baughman, R., J. Chem. Phys. 68, 5405 (1978); Baughman, R. H. and Hsu, S. L., Polym. Lett. 17, 185 (1979)

26. Mihály, L., Pekker, S. and Jánossy, A., J. of Synthetic Metals (in press)

27. Salaneck, W. R., Thomas, H. R., Bigelow, R. W., Duke, C. B., Plummer, E. W., Heeger, A. J. and MacDiarmid, A. G., J. Chem. Phys. (in press)

28. Salaneck, W. R., Thomas, H. R., Duke, C. B., Paton, A., Plummer, E. W., Heeger, A. J. and MacDiarmid, A. G., J. Chem. Phys. 71, 2044 (1979)

29. Fincher, C. R., Jr., Ozaki, M., Tanaka, M., Peebles, D. L., Lauchlan, L., Heeger, A. J. and MacDiarmid, A. G., Phys. Rev. B 20, 1589 (1979)

30. Park, Y. W., Denenstein, A., Chiang, C. K., Heeger, A. J. and MacDiarmid, A. G., Solid State Commun. 29, 747 (1979)

31. Kwak, J. F., Clarke, T. C., Greene, R. L. and Street, G. B., Solid State Commun. 31, 355 (1979)

32. Chiang, C. K., Park, Y. W., Heeger, A. J., Shirakawa, H., Louis, E. J. and MacDiarmid, A. G., J. Chem. Phys. 69, 5098 (1978)

33. Heikes, R., Buhl International Conference on Materials, edited by E. R. Shatz (Gordon and Breach, New York, 1974)

34. Chaikin, P. M. and Beni, G., Phys. Rev. B 13, 647 (1976)

35. Ozaki, M., Peebles, D. L., Weinberger, B. R., Heeger, A. J. and MacDiarmid, A. G. (to be published)

36. Mott, N. F., Philos. Mag. 19, 835 (1969); Mott, N. F., in Festkörperprobleme, edited by J. H. Queissen (Pergamon, New York, 1969), Vol. 9, p. 22; Ambegaokar, V., Halperin, B. I. and Langer, J. S., Phys. Rev. B 4, 2612 (1971)

37. Hsu, S. L., Signorelli, A. J., Pez, G. P. and Baughman, R. H., J. Chem. Phys. 69, 106 (1978); Shirakawa, H., Sasaki, T. and Ikeda, S., Chem. Lett. (Japan) p. 1113 (1978); Harada, I., Tasumi, M., Shirakawa, H. and Ikeda, S., Chem. Lett. (Japan) 1411 (1978)

38. As discussed above, the value $\rho_o \simeq 10^{-4}$ (2×10^{18} carriers per cm^3) for "undoped" trans-$(CH)_x$ was determined from the magnitude of the thermopower and independently verified from C vs V measurements on p-n heterojunctions. In our earlier paper (ref. 30) we estimated

$10^{-4} < \rho_o < 10^{-3}$ based on uncertainties at that time on the boundaries of the dilute regime. However, the insensitivity of the activation energy (ΔE) to y (see Fig. 4) below y = 0.001 clearly identifies this as the dilute regime. For y > 0.001, ΔE begins to fall dramatically indicative of the importance of dopant-dopant interactions. This independently demonstrates that ρ_o is well below 10^{-3} and implies that the number N of available sites is comparable to the number of carbon atoms per unit length in the polymer chain.

39. Montgomery, H. C., J. Appl. Phys. 42, 2971 (1971)

40. Thermoelectricity: An Introduction to the Principles, edited by D. K. C. MacDonald, (John Wiley and Sons, Inc., New York and London) p. 115

41. Mihály, G., Vancsó, G., Pekker, S. and Jánossy, A., J. of Synthetic Metals (in press)

42. Seeger, K., Gill, W. D., Clarke, T. C., Street, G. B., Solid State Commun. 28, 873 (1978)

43. Nechtschein, M., Devreux, F., Greene, R. L., Clarke, T. C. and Street, G. B., Phys. Rev. Lett. (Submitted)

44. Mott, N. F. and Twose, W. D., Adv. Phys. 10, 107 (1961); Borland, R. in Mathematical Physics in One Dimension, ed. by E. N. Lieb and D. C. Mattis (Acad. Press, N. Y., 1966) p. 319

45. Sheng, P., Sichel, E. K. and Gittleman, J. I., Phys. Rev. Lett. 40, 1197 (1978); Sichel, E. K., Gittleman, J. I. and Sheng, P., Phys. Rev. B 18, 5712 (1978); Sheng, P., Phys. Rev. B (Submitted)

46. Wnek, G. E., Chien, J. C. W., Karasz, F. E., Druy, M. A., Park, Y. W., MacDiarmid, A. G. and Heeger, A. J., J. Polymer Sci.; Polymer Letts. Ed. 17, 779 (1979)

47. Fincher, C. R., Jr., Ozaki, M., Heeger, A. J. and MacDiarmid, A. G., Phys. Rev. B 19, 4140 (1979)

48. Takayama, H., Lin-Liu, Y. R. and Maki, K., Phys. Rev. B (Submitted)

49. Wada, Y. and Schrieffer, J. R., Phys. Rev. B 18, 3897 (1978)

50. Ooshika, Y., J. Phys. Soc. Japan 12, pp. 1238, 1246 (1957)

Figure Captions:

Figure 1: Thermopower (S) vs y for $[CH(I_3)_y]_x$ at room temperature.

Figure 2: Temperature dependence of the thermopower in heavily doped metallic $[CH(AsF_5)_y]_x$

• • • $[CH(AsF_5)_{.147}]_x$: non-oriented

o o o $[CH(AsF_5)_{.095}]_x$: oriented, $\ell/\ell = 3.2$

Figure 3: Conductivity vs $\frac{1}{T}$ for $[CH(AsF_5)_y]_x$ for values of y spanning the full doping regime.

Δ Δ Δ oriented sample ($\ell/\ell_o = 3.1$) y = 0.14

o o o non-oriented with y as indicated.

Figure 4: Activation energy vs y for $[CH(AsF_5)_y]_x$ and $[CH(I_3)_y]_x$.

o o o trans-$[CH(AsF_5)_y]_x$; data obtained from Fig. 3.

• • • trans-$[CH(I_3)_y]_x$; data obtained from ref. 35.

Figure 5: Room temperature conductivity vs y, in the dilute limit, for $[CH(AsF_5)_y]_x$. The solid line has slope of unity indicating that initially σ is approximately proportional to y.

Figure 6: Temperature dependence of the normalized conductivity of heavily doped metallic $(CH)_x$

• • • $[CH(AsF_5)_{0.14}]_x$; $\sigma_{RT} = 2450\ \Omega^{-1}\text{-cm}^{-1}$

o o o $[CH(I_3)_{.08}]_x$; $\sigma_{RT} = 1500\ \Omega^{-1}\text{-cm}^{-1}$

Both samples were made from oriented cis starting material with $\ell/\ell_o = 3.1$.

Figure 7: Low temperature conductivity of the metallic samples of Figure 6.

Figure 8: Temperature dependence of normalized conductivity of metallic <u>trans</u>-$[CH(AsF_5)_{0.10}]_x$

+ $\sigma_{||}$ with $\ell/\ell_o = 2.8$ $\sigma_{||}(RT) = 1400\ \Omega^{-1}\text{-cm}^{-1}$

x $\sigma_{\perp}$ with $\ell/\ell_o = 2.8$ $\sigma_{\perp}(RT) = 280\ \Omega^{-1}\text{-cm}^{-1}$

• $\sigma_{||}$ with $\ell/\ell_o = 1$ $\sigma_{||}(RT) = 240\ \Omega^{-1}\text{-cm}^{-1}$

o $\sigma_{\perp}$ with $\ell/\ell_o = 1$ $\sigma_{\perp}(RT) = 230\ \Omega^{-1}\text{-cm}^{-1}$

The data marked $\sigma_{||}$ and $\sigma_{\perp}$ for $\ell/\ell_o = 1$ (unstretched) represent two independent samples cut at 90° from a non-oriented film.

Figure 9: Low temperature conductivity of the metallic sample of Figure 8.

Figure 10: Normalized temperature dependence of <u>trans</u>-$[CH(AsF_5)_y]_x$ for $\ell/\ell_o = 3.0$.

Δ Δ Δ $y = 0$

x x x $y = 0.004$

• • • $y = 0.008$

o o o $y = 0.03$

+ + + $y = 0.10$

Figure 11: Low temperature conductivity (normalized) vs concentration. The onset of finite conductivity vs $T \rightarrow 0$ is indicative of the semiconductor-metal transition

Figure 12: Transport mobility vs concentration (see text).

• • • <u>trans</u>-$[CH(AsF_5)_y]_x$

o o o <u>trans</u>-$[CH(I_3)_y]_x$

Figure 13: $-[\ell n \sigma/\sigma_{RT}]^{-1}$ vs T; this plot allows evaluation of the junction barrier parameters (see text).

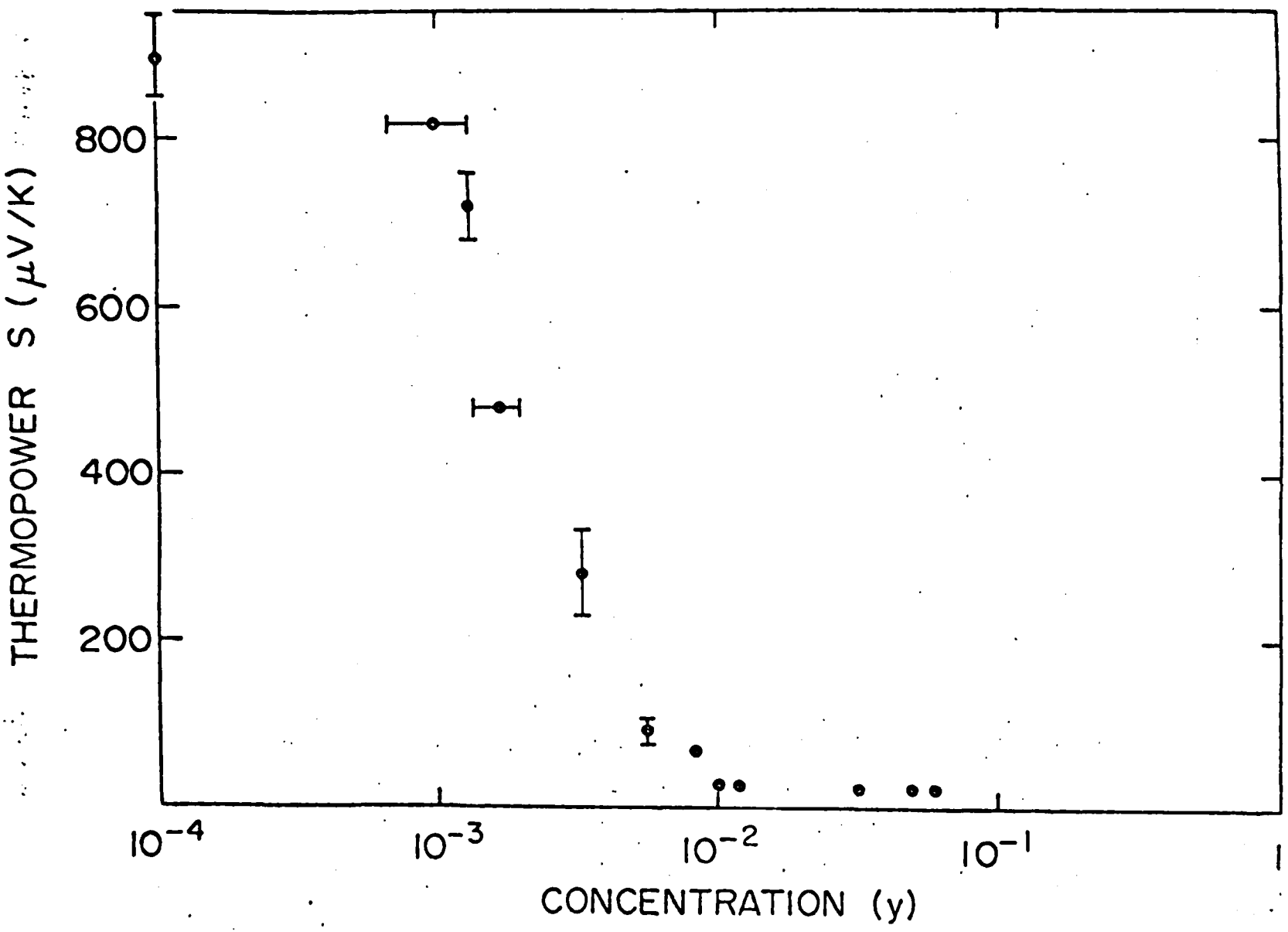

Figure 1: Thermopower (S) vs y for $[CH(I_3)_y]_x$ at room temperature.

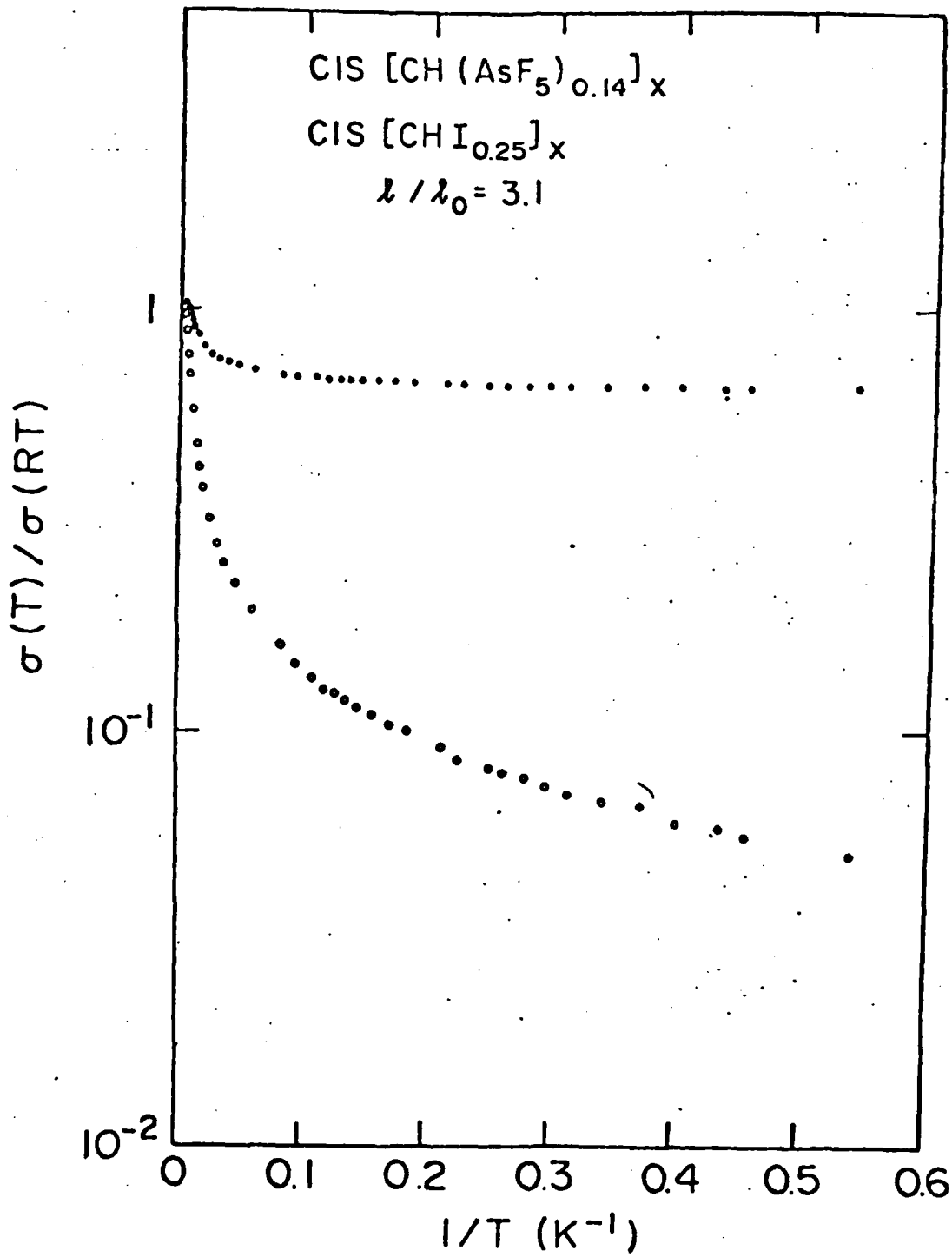

Figure 7: Low temperature conductivity of the metallic samples of Figure 6.

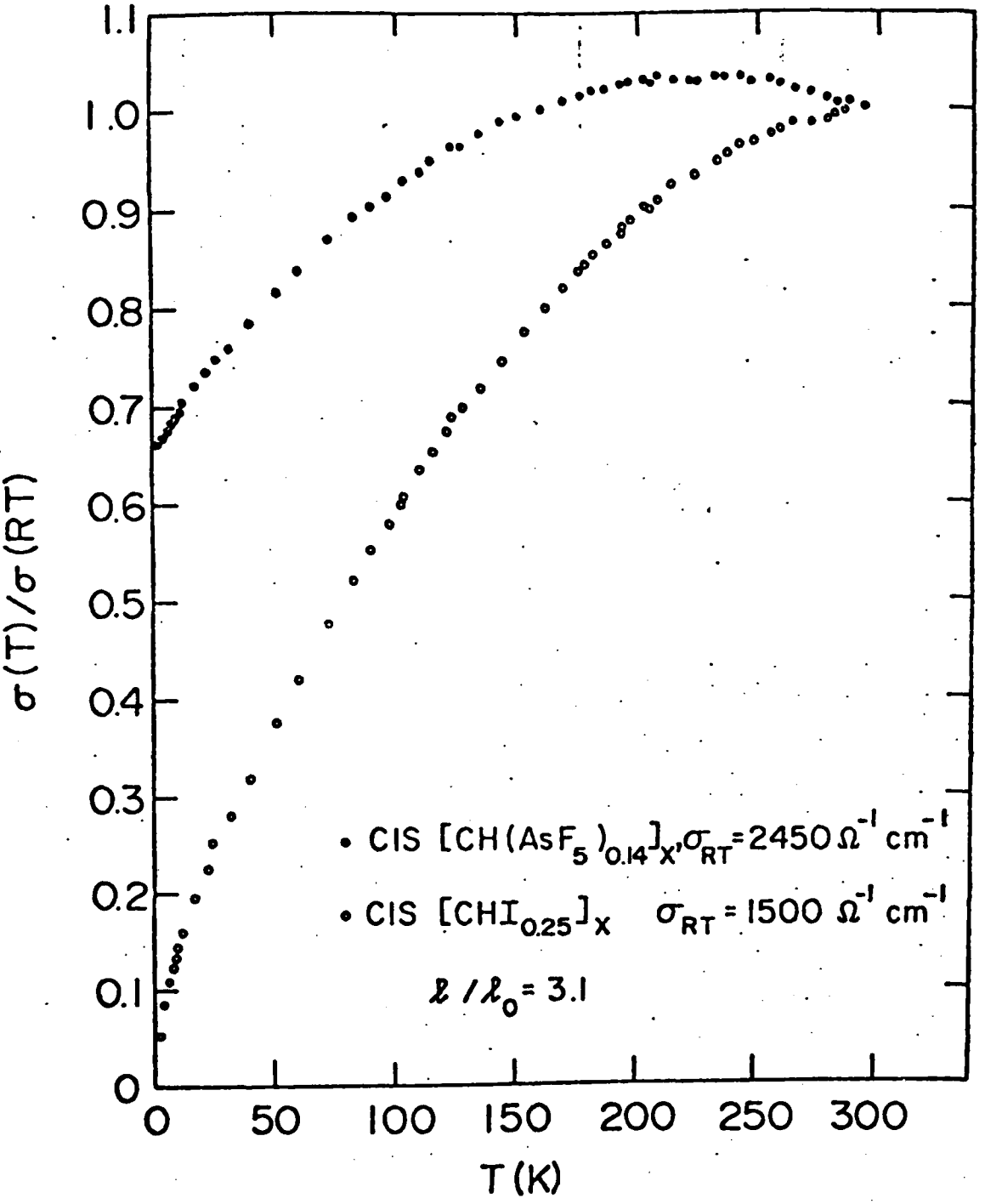

Figure 6: Temperature dependence of the normalized conductivity of heavily doped metallic $(CH)_x$

• • • $[CH(AsF_5)_{0.14}]_x$; $\sigma_{RT} = 2450\ \Omega^{-1}\text{-cm}^{-1}$

o o o $[CH(I_3)_{.08}]_x$; $\sigma_{RT} = 1500\ \Omega^{-1}\text{-cm}^{-1}$

Both samples were made from oriented <u>cis</u> starting material with $\ell/\ell_0 = 3.1$.

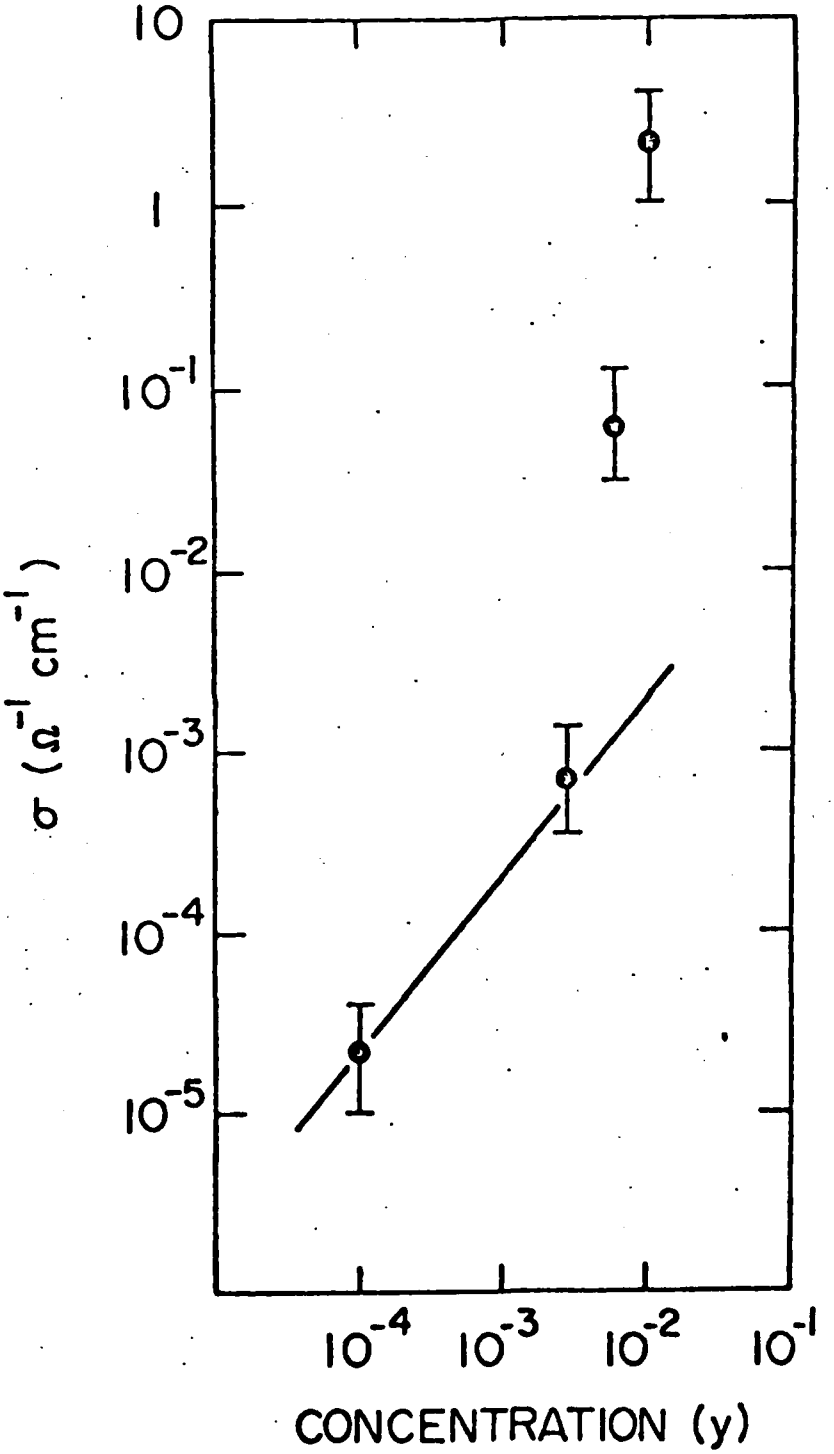

Figure 5: Room temperature conductivity vs y, in the dilute limit, for $[CH(AsF_6)_y]_x$. The solid line has slope of unity indicating that initially σ is approximately proportional to y.

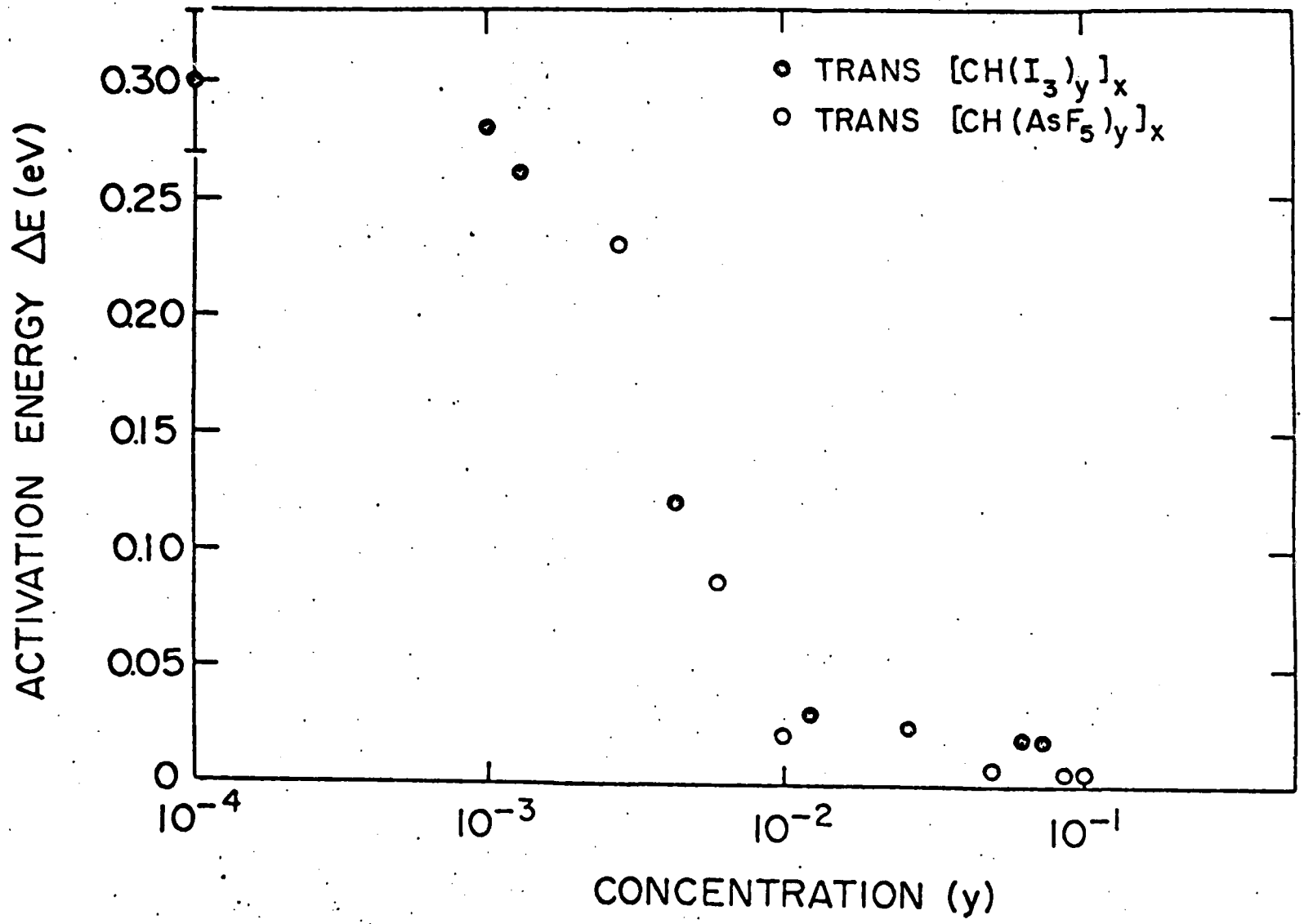

Figure 4: Activation energy vs y for $[CH(AsF_6)_y]_x$ and $[CH(I_3)_y]_x$.

o o o <u>trans</u>-$[CH(AsF_6)_y]_x$: data obtained from Fig. 3.

• • • <u>trans</u>-$[CH(I_3)_y]_x$: data obtained from ref. 35.

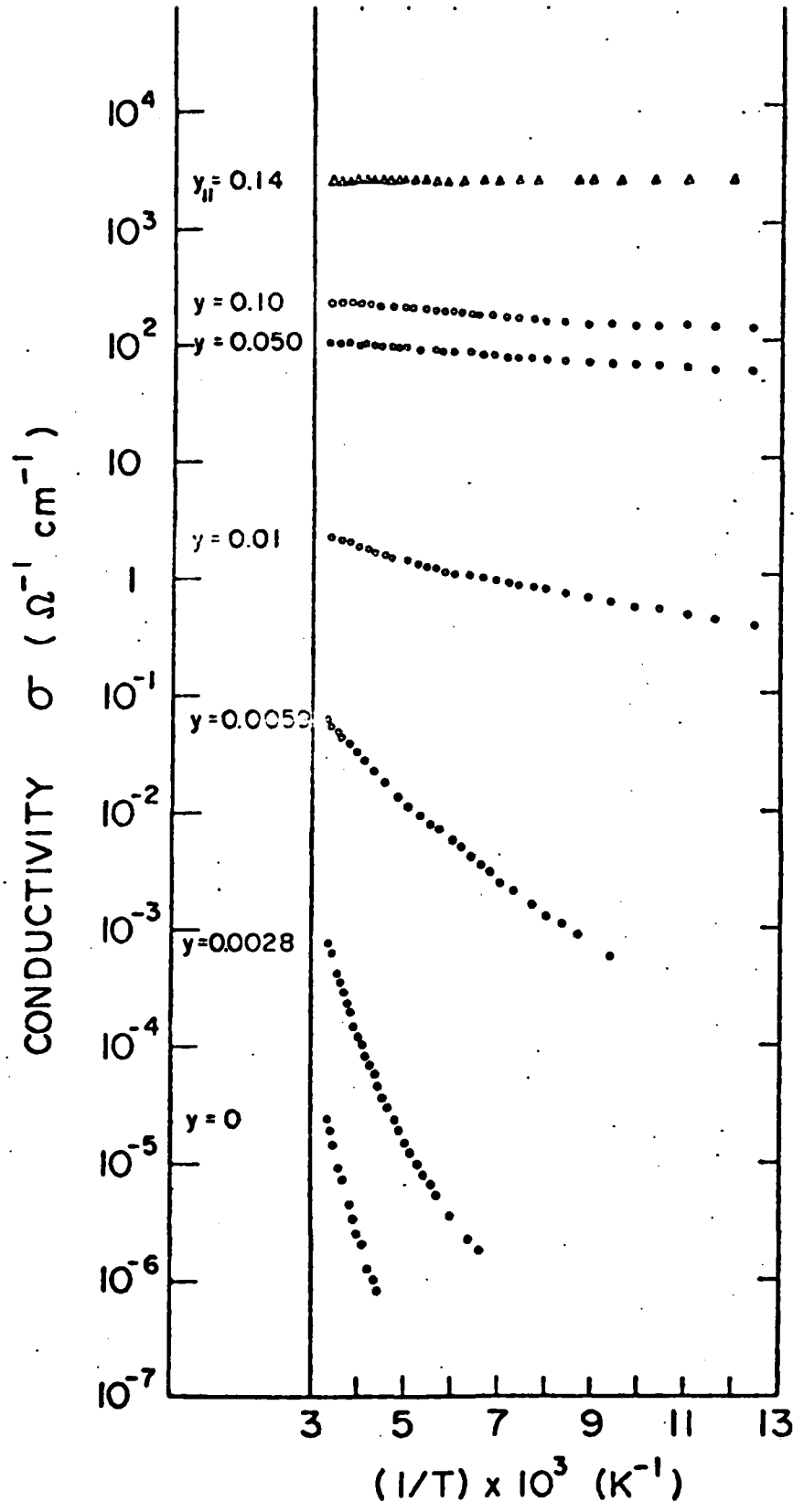

Figure 3: Conductivity vs $\frac{1}{T}$ for $[CH(AsF_6)_y]_x$ for values of y spanning the full doping regime.

Δ Δ Δ oriented sample (ℓ/ℓ_o = 3.1) y = 0.14

o o o non-oriented with y as indicated.

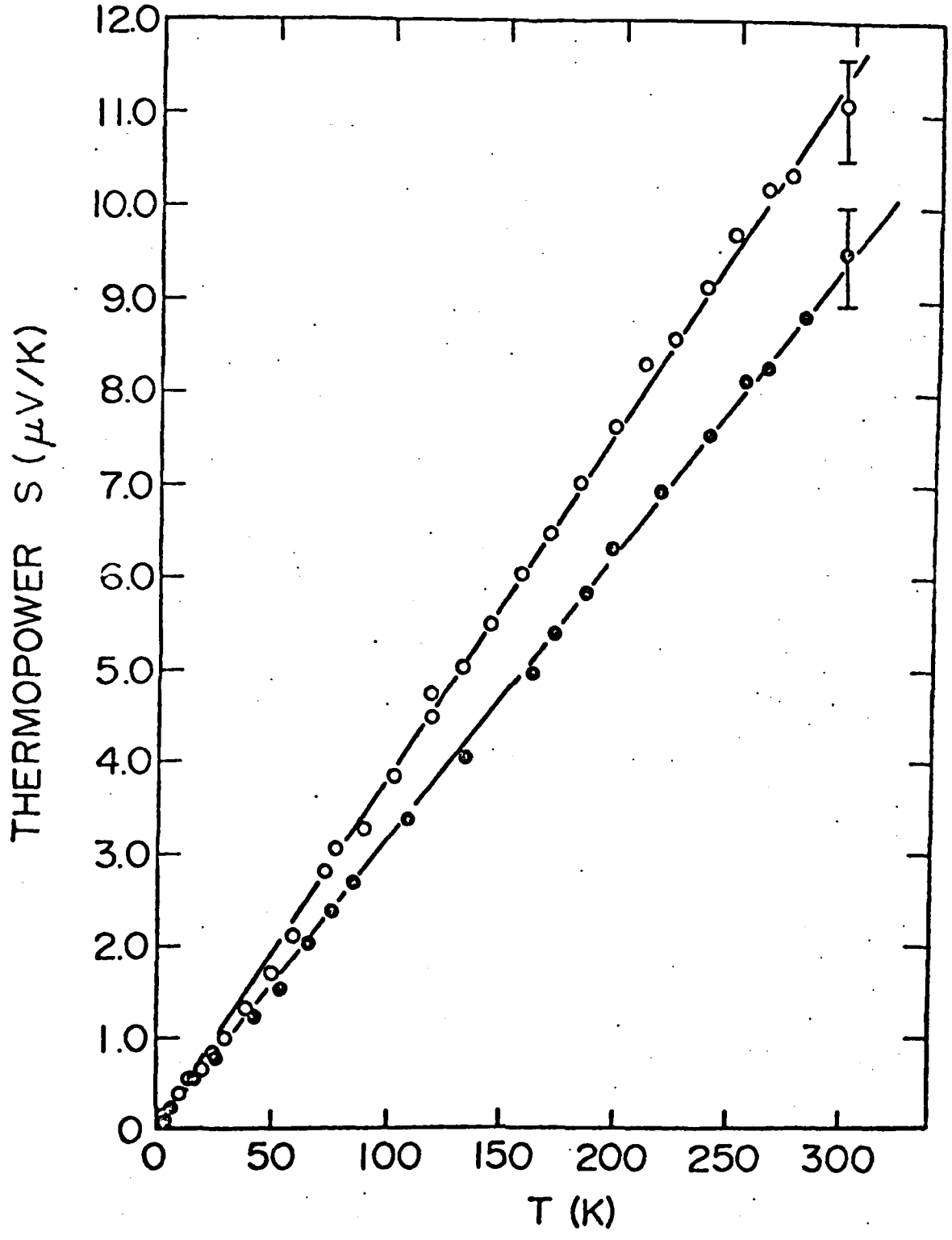

Figure 2: Temperature dependence of the thermopower in heavily doped metallic $[CH(AsF_5)_y]_x$

• • • $[CH(AsF_5)_{.147}]_x$: non-oriented

o o o $[CH(AsF_5)_{.095}]_x$: oriented, $l/t = 3.2$

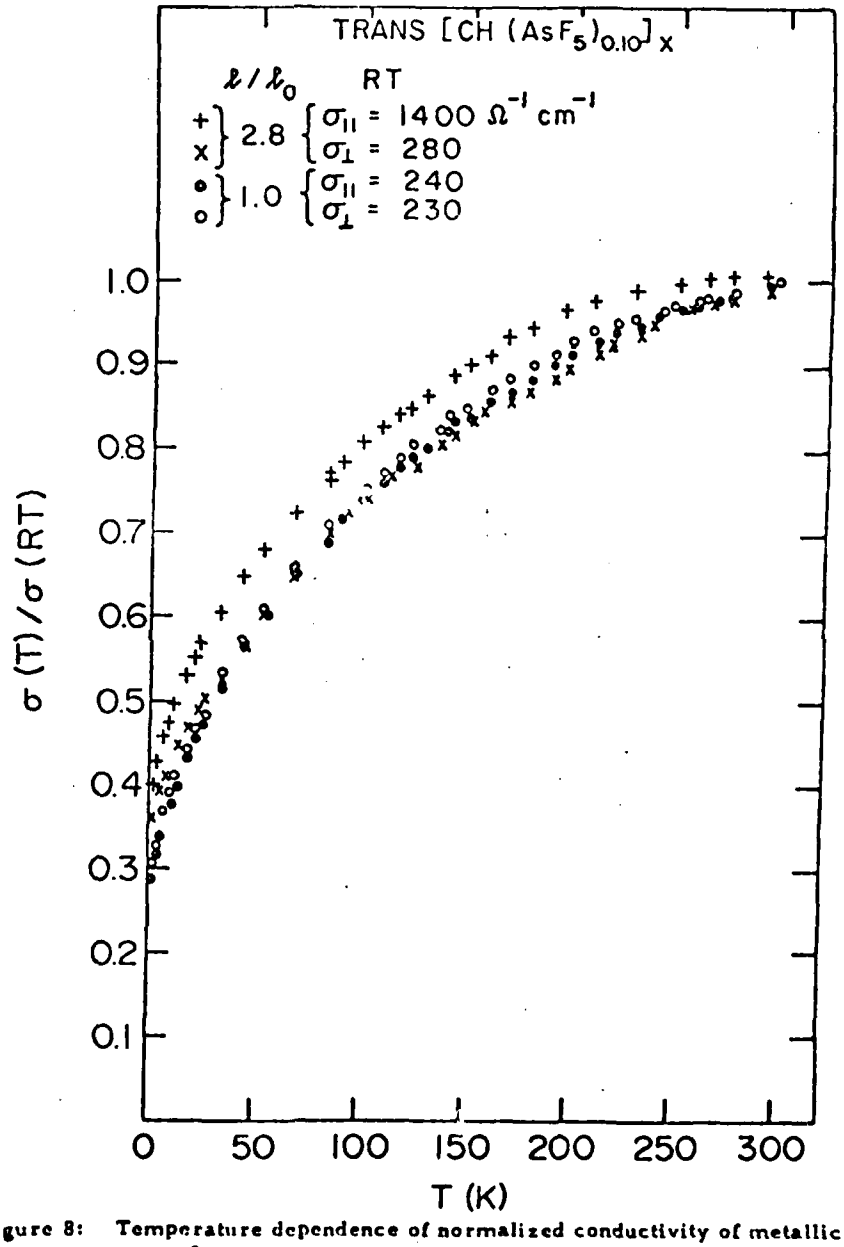

Figure 8: Temperature dependence of normalized conductivity of metallic trans-$[CH(AsF_5)_{0.10}]_x$

+ $\sigma_{\parallel}$ with $\ell/\ell_o = 2.8$ $\sigma_{\parallel}(RT) = 1400\ \Omega^{-1}\text{-cm}^{-1}$

x $\sigma_{\perp}$ with $\ell/\ell_o = 2.8$ $\sigma_{\perp}(RT) = 280\ \Omega^{-1}\text{-cm}^{-1}$

• $\sigma_{\parallel}$ with $\ell/\ell_o = 1$ $\sigma_{\parallel}(RT) = 240\ \Omega^{-1}\text{-cm}^{-1}$

o $\sigma_{\perp}$ with $\ell/\ell_o = 1$ $\sigma_{\perp}(RT) = 230\ \Omega^{-1}\text{-cm}^{-1}$

The data marked $\sigma_{\parallel}$ and $\sigma_{\perp}$ for $\ell/\ell_o = 1$ (unstretched) represent two independent samples cut at 90° from a non-oriented film.

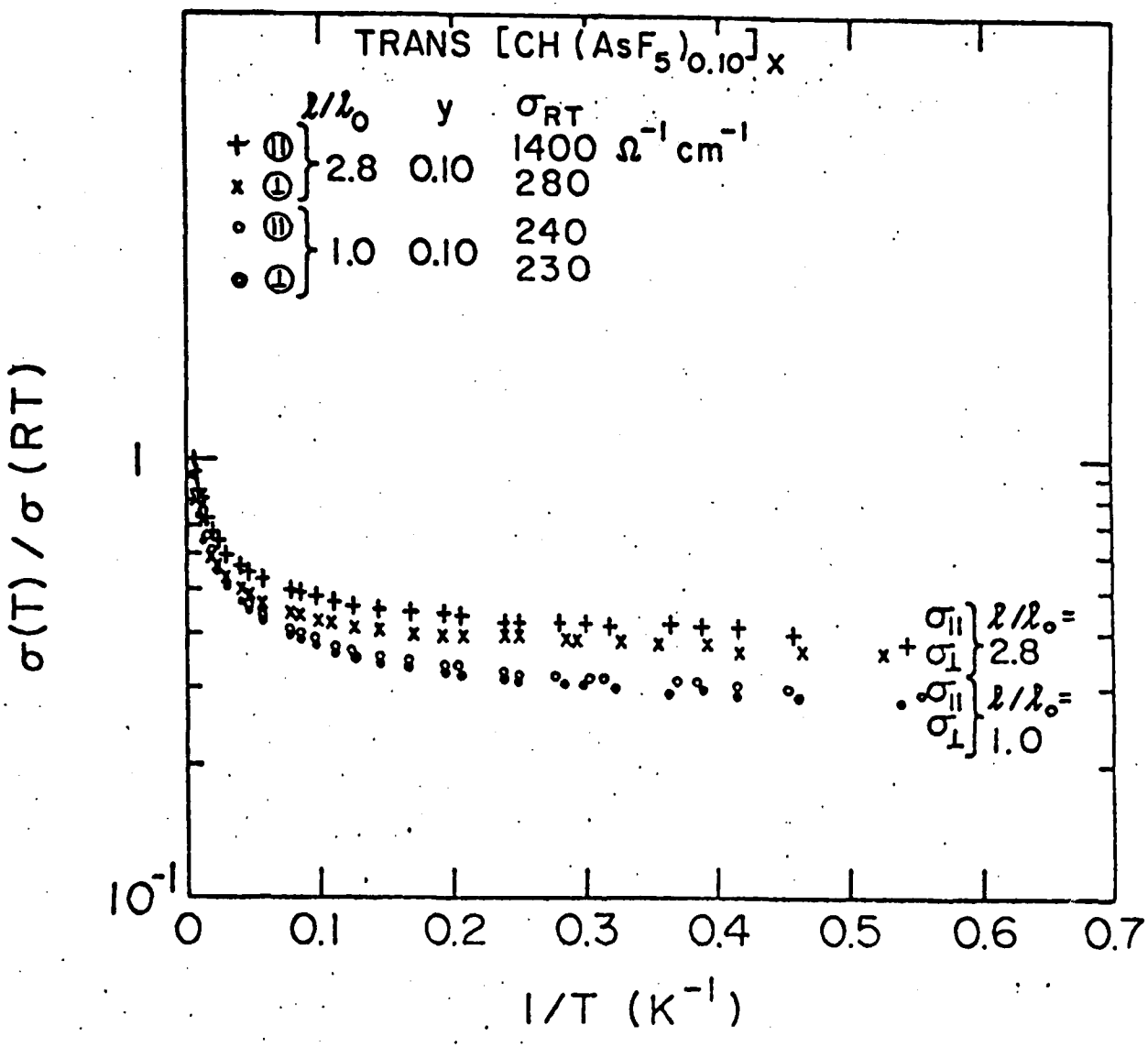

Figure 9: Low temperature conductivity of the metallic sample of Figure 8.

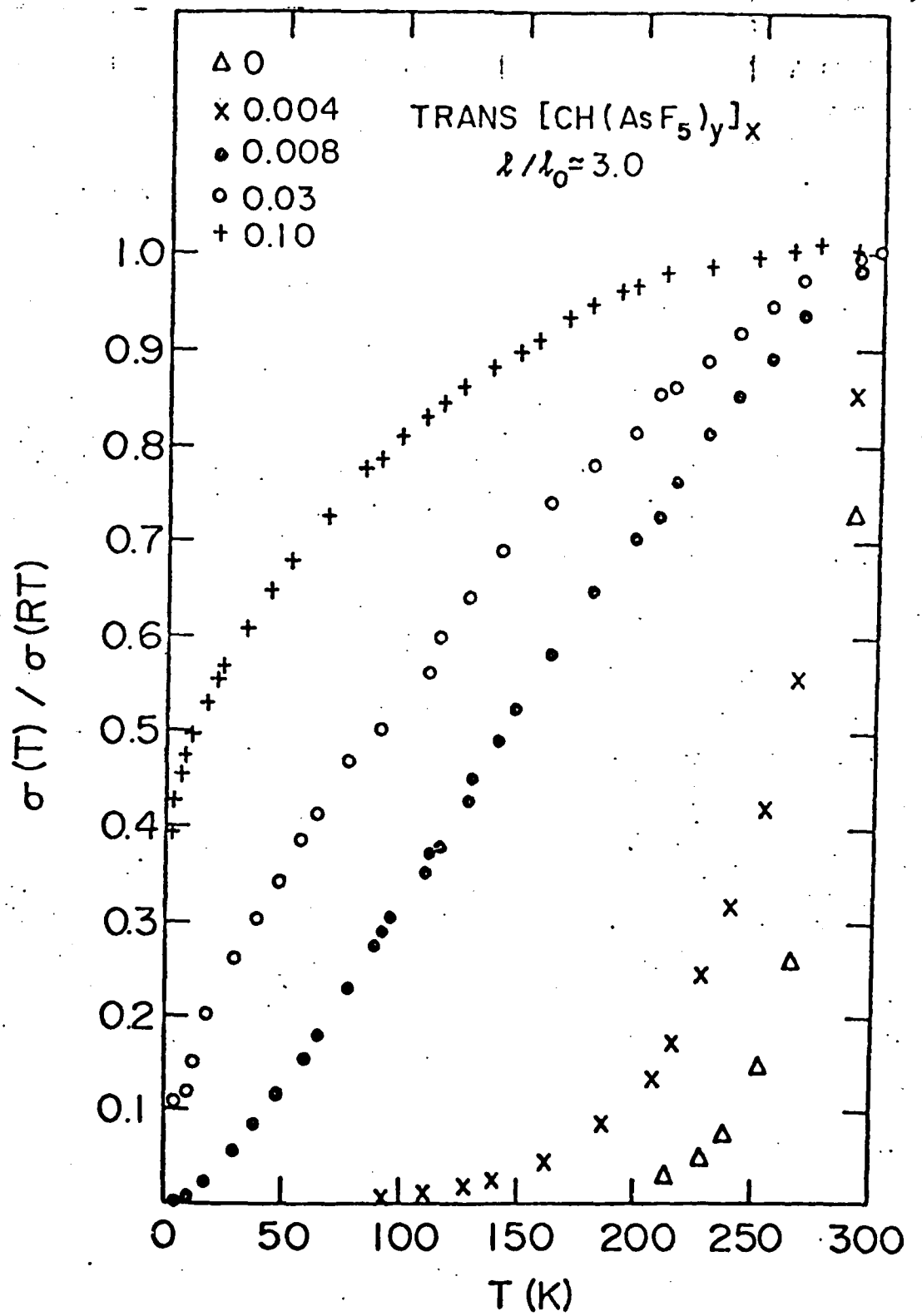

Figure 10: Normalized temperature dependence of <u>trans</u>-$[CH(AsF_5)_y]_x$ for $l/l_o = 3.0$.

Δ Δ Δ	y = 0
x x x	y = 0.004
• • •	y = 0.008
o o o	y = 0.03
+ + +	y = 0.10

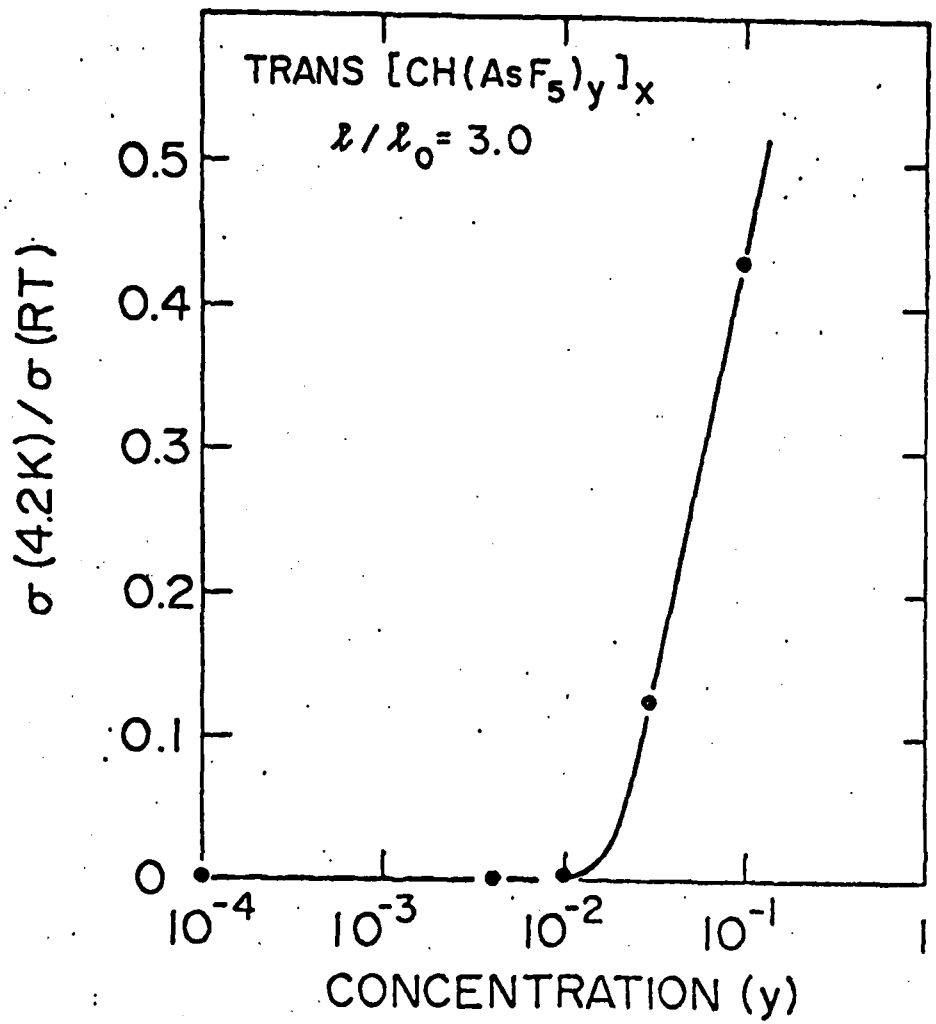

Figure 11: Low temperature conductivity (normalized) vs concentration. The onset of finite conductivity vs T → 0 is indicative of the semiconductor-metal transition

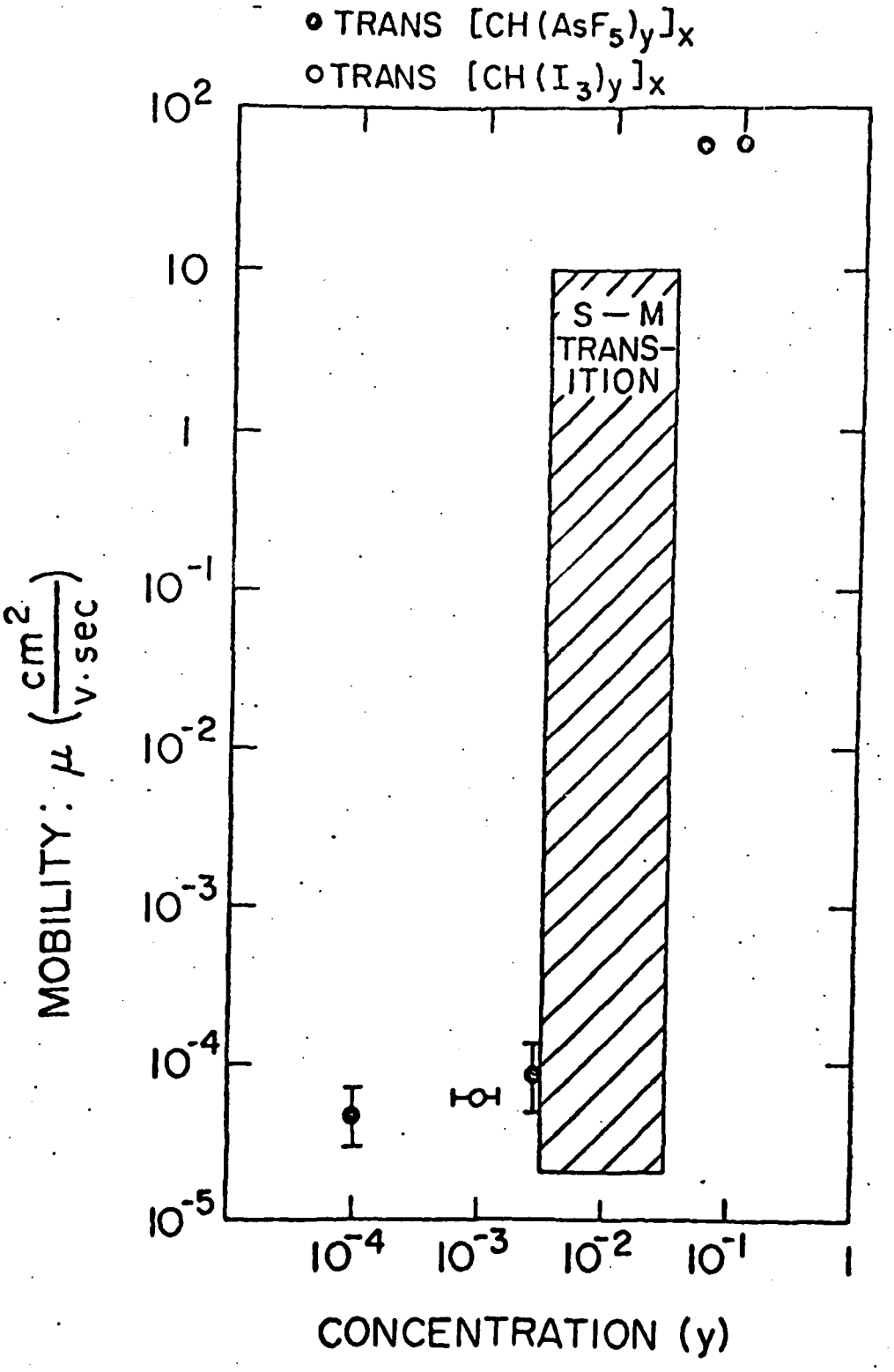

Figure 12: Transport mobility vs concentration (see text).

• • • trans-$[CH(AsF_5)_y]_x$

o o o trans-$[CH(I_3)_y]_x$

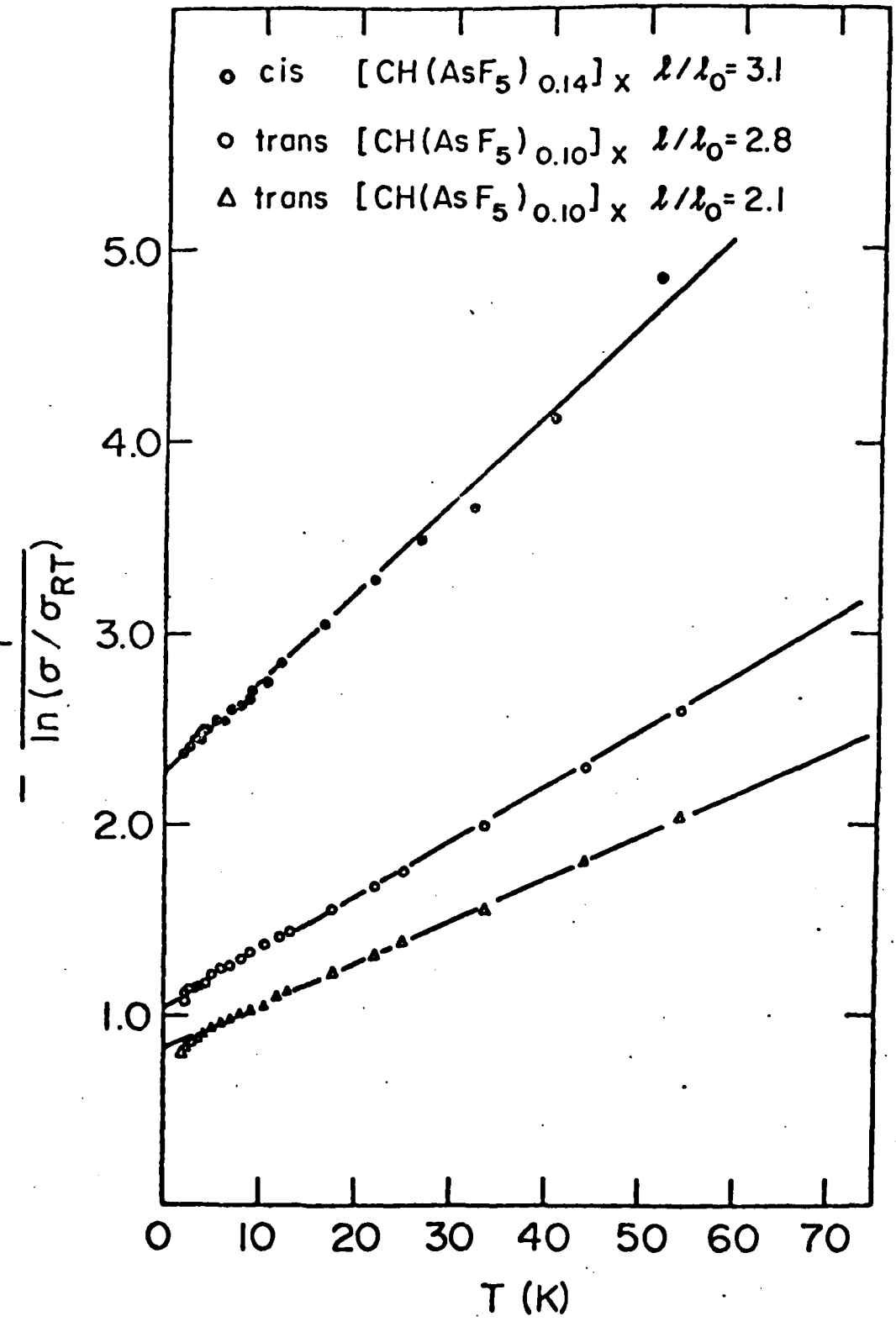

Figure 13: $-[\ln\sigma/\sigma_{RT}]^{-1}$ **vs T; this plot allows evaluation of the junction barrier parameters (see text).**

TECHNICAL REPORT DISTRIBUTION LIST, GEN

	No. Copies
Office of Naval Research Attn: Code 472 800 North Quincy Street Arlington, Virginia 22217	2
ONR Branch Office Attn: Dr. George Sandoz 536 S. Clark Street Chicago, Illinois 60605	1
ONR Branch Office Attn: Scientific Dept. 715 Broadway New York, New York 10003	1
ONR Branch Office 1030 East Green Street Pasadena, California 91106	1
ONR Branch Office Attn: Dr. L. H. Peebles Building 114, Section D 666 Summer Street Boston, Massachusetts 02210	1
Director, Naval Research Laboratory Attn: Code 6100 Washington, D.C. 20390	1
The Assistant Secretary of the Navy (R,E&S) Department of the Navy Room 4E736, Pentagon Washington, D.C. 20350	1
Commander, Naval Air Systems Command Attn: Code 310C (H. Rosenwasser) Department of the Navy Washington, D.C. 20360	1
Defense Documentation Center Building 5, Cameron Station Alexandria, Virginia 22314	12
Dr. Fred Saalfeld Chemistry Division Naval Research Laboratory Washington, D.C. 20375	1
U.S. Army Research Office Attn: CRD-AA-IP P.O. Box 1211 Research Triangle Park, N.C. 27709	1
Naval Ocean Systems Center Attn: Mr. Joe McCartney San Diego, California 92152	1
Naval Weapons Center Attn: Dr. A. B. Amster, Chemistry Division China Lake, California 93555	1
Naval Civil Engineering Laboratory Attn: Dr. R. W. Drisko Port Hueneme, California 93401	1
Department of Physics & Chemistry Naval Postgraduate School Monterey, California 93940	1
Dr. A. L. Slafkosky Scientific Advisor Commandant of the Marine Corps (Code RD-1) Washington, D.C. 20380	1
Office of Naval Research Attn: Dr. Richard S. Miller 800 N. Quincy Street Arlington, Virginia 22217	1
Naval Ship Research and Development Center Attn: Dr. G. Bosmajian, Applied Chemistry Division Annapolis, Maryland 21401	1
Naval Ocean Systems Center Attn: Dr. S. Yamamoto, Marine Sciences Division San Diego, California 91232	1
Mr. John Boyle Materials Branch Naval Ship Engineering Center Philadelphia, Pennsylvania 19112	1

472:GAN:716:at
78u472-608

TECHNICAL REPORT DISTRIBUTION LIST, 356B

	No. Copies
Dr. T. C. Williams Union Carbide Corporation Chemical and Plastics Tarrytown Technical Center Tarrytown, New York	1
Dr. R. Soulen Contract Research Department Pennwalt Corporation 900 First Avenue King of Prussia, Pennsylvania 19406	1
Dr. A. G. MacDiarmid University of Pennsylvania Department of Chemistry Philadelphia, Pennsylvania 19174	1
Dr. C. Pittman University of Alabama Department of Chemistry University, Alabama 35486	1
Dr. H. Allcock Pennsylvania State University Department of Chemistry University Park, Pennsylvania 16802	1
Dr. M. Kenney Case-Western University Department of Chemistry Cleveland, Ohio 44106	1
Dr. R. Lenz University of Massachusetts Department of Chemistry Amherst, Massachusetts 01002	1
Dr. M. David Curtis University of Michigan Department of Chemistry Ann Arbor, Michigan 48105	1
Dr. M. Good Division of Engineering Research Louisiana State University Baton Rouge, Louisiana 70803	1
Douglas Aircraft Company 3855 Lakewood Boulevard Long Beach, California 90846 Attn: Technical Library C1 290/36-84 AUTO-Sutton	1
NASA-Lewis Research Center 21000 Brookpark Road Cleveland, Ohio 44135 Attn: Dr. T. T. Serafini, MS 49-1	1
Dr. J. Griffith Naval Research Laboratory Chemistry Section, Code 6120 Washington, D.C. 20375	
Dr. G. Goodman Globe-Union Incorporated 5757 North Green Bay Avenue Milwaukee, Wisconsin 53201	1
Dr. E. Fischer, Code 2853 Naval Ship Research and Development Center Annapolis Division Annapolis, Maryland 21402	1
Dr. Martin H. Kaufman, Head Materials Research Branch (Code 4542) Naval Weapons Center China Lake, California 93555	1
Dr. J. Magill University of Pittsburg Metallurgical and Materials Engineering Pittsburg, Pennsylvania 22230	1
Dr. C. Allen University of Vermont Department of Chemistry Burlington, Vermont 05401	1
Dr. D. Bergbreiter Texas A&M University Department of Chemistry College Station, Texas 77843	1

472:GAN:716:ah
78u472-608

TECHNICAL REPORT DISTRIBUTION LIST, 356B

	No. Copies
Professor R. Drago Department of Chemistry University of Illinois Urbana, Illinois 61801	1
Dr. F. Brinkman Chemical Stability & Corrosion Division Department of Commerce National Bureau of Standards Washington, D.C. 20234	1
Professor H. A. Titus Department of Electrical Engineering Naval Postgraduate School Monterey, California 93940	1
COL B. E. Clark, Code 100M Office of Naval Research 800 N. Quincy Street Arlington, Virginia 22217	1
Professor T. Katz Department of Chemistry Columbia University New York, New York 10027	1
Dr. Frank Karasz Department of Polymer Science and Engineering University of Massachusetts Amherst, Massachusetts 01003	1
Dr. James Chien Department of Polymer Science and Engineering University of Massachusetts Amherst, Massachusetts 01003	1
Professor A. J. Heeger Director Laboratory for Research on Structure of Matter 33rd and Walnut Streets/K1 University of Pennsylvania Philadelphia, Pennsylvania 19104	1
Dr. Richard A. Reynolds Deputy Director Defense Sciences Office DARPA 1400 Wilson Blvd. Arlington, Virginia 22209	1
Dr. Rudolph J. Marcus Office of Naval Research Scientific Liaison Group American Embassy APO San Francisco 96503	1
Mr. James Kelley DTNSRDC Code 2803 Annapolis, Maryland 21402	1